



## **Towards a Standard for Vessel URN Measurement in Shallow Water**

---

**Applying Acoustical Propagation Modelling to Inform the Design of a  
Measurement Program that Determines if Shallow Water URN Measurements  
can be Comparable to those from Deep Water**

Submitted to:

Véronique Nolet  
Transport Canada Innovation Center  
*Contract: T8009-190191/002/XLV*

Authors:

Michael A. Ainslie  
S. Bruce Martin  
Terry J. Deveau  
Alexander O. MacGillivray  
Chanwoo Bae (BC Ferries)  
Dietrich Wittekind (DW-ShipConsult)

18 August 2021

P001556-002  
Document 02167  
Version 1.0

JASCO Applied Sciences (Canada) Ltd  
Suite 2305, 4464 Markham St.  
Victoria, BC V8Z 7X8 Canada  
Tel: +1-250-483-3300  
Fax: +1-250-483-3301  
[www.jasco.com](http://www.jasco.com)



**Suggested citation:**

Ainslie, M.A., S.B. Martin, T.J. Deveau, A.O. MacGillivray, C. Bae, and D. Wittekind. 2020. *Towards a Standard for Vessel URN Measurement in Shallow Water: Applying Acoustical Propagation Modelling to Inform the Design of a Measurement Program that Determines if Shallow Water URN Measurements can be Comparable to those from Deep Water*. Document 02167, Version 1.0. White paper by JASCO Applied Sciences for Transport Canada Innovation Center.

**Disclaimer:**

The results presented herein are relevant within the specific context described in this report. They could be misinterpreted if not considered in the light of all the information contained in this report. Accordingly, if information from this report is used in documents released to the public or to regulatory bodies, such documents must clearly cite the original report, which shall be made readily available to the recipients in integral and unedited form.



Transport  
Canada

Transports  
Canada

## PUBLICATION DATA FORM

1. Transport Canada Publication No. <b>TP 15483E</b>		2. Project No. <b>MMP2</b>		3. Recipient's Catalogue No.	
4. Title and Subtitle <b>Towards a Standard for Vessel URN Measurement in Shallow Water</b>				5. Publication Date <b>2021-07-08</b>	
				6. Performing Organization Document No. <b>02167</b>	
7. Author(s) <b>Michael A. Ainslie, S. Bruce Martin, Terry J. Deveau, Alexander O. MacGillivray, Chanwoo Bae (BC Ferries), Dietrich Wittekind (DW-ShipConsult)</b>				8. Transport Canada File No. <b>-</b>	
9. Performing Organization Name and Address <b>JASCO Applied Sciences (Canada) Ltd. 2305-4464 Markham Street Victoria, BC V8Z 7X8 Canada</b>				10. PWGSC File No. <b>-</b>	
				11. PWGSC or Transport Canada Contract No. <b>T8009-190191/002</b>	
12. Sponsoring Agency Name and Address <b>Transport Canada, Innovation Centre Place de Ville, Tower C 330 Sparks Street, Ottawa ON K1A 0N5</b>				13. Type of Publication and Period Covered <b>Technical Report, 2020-2021</b>	
				14. Project Officer <b>Veronique Nolet</b>	
15. Supplementary Notes (Funding programs, titles of related publications, etc.) <b>This project was funded under the Marine RD&amp;D program</b>					
16. Abstract <p>JASCO Applied Sciences, in collaboration with BC Ferries (BCF) and DW-ShipConsult, are executing a project sponsored by Transport Canada's Innovation Center (TC-IC) to provide results that will assist the International Standards Organization (ISO) in developing standard 17208-3 for the measurement of vessel underwater radiated noise (URN) in shallow water. Measurements in shallow water are difficult to perform because of the ways in which sound interacts with the seafloor and sea surface.</p> <p>In assisting the ISO to develop standard 17208-3, this project aims to answer the question: What combination of sensors and analysis methods yield measurements of vessel underwater sound levels in shallow water consistent with those that are known to be accurately obtained in deep water using ISO Standard 17208-1/-2? The project has two phases: 1) development of a white paper that describes the issues associated with shallow water vessel sound level measurements and an associated measurement plan that address the identified knowledge gaps and 2) execution of the experiments and analysis of the collected measurements to address the knowledge gaps. Experimental measurements will be performed in shallow, mid, and deep water on the same BCF route (Tsawwassen to Swartz Bay).</p> <p>The scope of this white paper is to analyze and illustrate the issues that complicate vessel URN measurements in shallow water, for the purpose of eliciting feedback from TC-IC and members of the ISO committee developing 17208-3 (Technical Committee (TC) 43, Subcommittee (SC) 3, Working Group (WG) 1 – TC 43/SC 3/WG 1). The white paper first provides an overview of the issues associated with making shallow water URN measurements; it then documents the results of acoustic propagation modeling numerical experiments that provide insight into where to measure, the appropriateness of different analysis techniques, and effects of sea bottom composition. The exposition concludes with recommendations for the hydrophone geometries to employ for at-sea measurements that will be performed in summer 2021.</p> <p>After publication of this white paper, measurements using prototype moorings will be made in coastal waters off Halifax, NS. The input received from ISO TC 43/SC 3/WG 1 and the results of the prototype experiment will inform the development of the final measurement plan, which will be reviewed with ISO TC 43/SC 3/WG 1 in December 2020 to elicit further feedback and comments.</p>					
17. Key Words <b>Underwater Radiated Noise</b>			18. Distribution Statement <b>Digital Copy</b>		
19. Security Classification (of this publication) <b>Unclassified</b>	20. Security Classification (of this page) <b>Unclassified</b>	21. Declassification (date) <b>—</b>	22. No. of Pages <b>65</b>	23. Price <b>Shipping/ Handling</b>	



1. N° de la publication de Transports Canada <b>TP 15483E</b>		2. N° de l'étude <b>MMP2</b>		3. N° de catalogue du destinataire	
4. Titre et sous-titre <b>Vers une norme pour la mesure de l'URN des navires en eaux peu profondes</b>				5. Date de la publication <b>2021-07-08</b>	
				6. N° de document de l'organisme exécutant <b>02167</b>	
7. Auteur(s) <b>Michael A. Ainslie, S. Bruce Martin, Terry J. Deveau, Alexander O. MacGillivray, Chanwoo Bae (BC Ferries), Dietrich Wittekind (DW-ShipConsult)</b>				8. N° de dossier - Transports Canada <b>-</b>	
9. Nom et adresse de l'organisme exécutant <b>JASCO Applied Sciences (Canada) Ltd. 2305-4464 Markham Street Victoria, BC V8Z 7X8 Canada</b>				10. N° de dossier - TPSGC <b>-</b>	
				11. N° de contrat - TPSGC ou Transports Canada <b>T8009-190191/002</b>	
12. Nom et adresse de l'organisme parrain <b>Centre d'innovation (IC) Place de Ville, tour C 330 rue Sparks Ottawa (Ontario) K1A 0N5</b>				13. Genre de publication et période visée <b>Rapport technique, 2020-2021</b>	
				14. Agent de projet <b>Veronique Nolet</b>	
15. Remarques additionnelles (programmes de financement, titres de publications connexes, etc.)					
16. Résumé <p>JASCO Applied Sciences (en collaboration avec BC Ferries et DW-ShipConsult) réalise actuellement un projet parrainé par le Centre d'innovation de Transports Canada en vue d'obtenir des résultats qui aideront l'Organisation internationale de normalisation à élaborer la norme 17208-3 pour le mesurage de l'acoustique sous-marine des navires en eau peu profonde. Le mesurage du bruit en eau peu profonde est difficile à effectuer en raison de la façon dont il interagit avec le fond marin et la surface de la mer.</p> <p>Pour aider l'Organisation internationale de normalisation à élaborer la norme 17208-3, ce projet vise à répondre à la question : quelle combinaison de capteurs et de méthodes d'analyse produisent un mesurage de l'acoustique sous-marine des navires en eau peu profonde concordant avec celui qui est obtenu de façon exacte en eau profonde à l'aide de la norme 17208-1/-2 de l'Organisation internationale de normalisation? Le projet est composé de deux étapes : premièrement, l'élaboration d'un livre blanc décrivant les enjeux relatifs au mesurage de l'acoustique sous-marine des navires en eau peu profonde et le plan connexe de mesurage visant à combler les lacunes connues en matière de connaissances, et, deuxièmement, l'expérimentation et l'analyse des mesures recueillies en vue de combler les lacunes en matière de connaissances. Le mesurage expérimental sera réalisé en eau peu profonde, en eau intermédiaire et en eau profonde sur un même trajet de BC Ferries (de Tsawwassen à Swartz Bay).</p> <p>L'objet du livre blanc est d'analyser et d'illustrer les enjeux qui compliquent le mesurage de l'acoustique sous-marine des navires en eau peu profonde dans le but de solliciter une rétroaction du Centre d'innovation de Transports Canada et des membres du comité de l'Organisation internationale de normalisation responsable de l'élaboration de la norme 17208-3 (comité technique [CT] 43, sous-comité [SC] 3, groupe de travail [GT] 1 : CT 43/SC 3/GT 1). Le livre blanc offre un aperçu des enjeux relatifs au mesurage du bruit sous-marin rayonné par les navires en eau peu profonde; il documente ensuite les résultats de l'expérimentation de la modélisation numérique de la propagation acoustique donnant un aperçu des endroits où mesurer, du caractère approprié de différentes techniques d'analyse, et des incidences de la composition du fond marin. L'exposition se termine avec des recommandations quant aux configurations géométriques des hydrophones à employer pour les mesures en mer qui seront réalisées à l'été 2021.</p> <p>Après la publication du livre blanc, un mesurage sera réalisé à l'aide de prototypes d'amarrages dans les eaux côtières au large de Halifax (Nouvelle-Écosse). La rétroaction du CT 43/SC 3/GT 1 de l'Organisation internationale de normalisation et les résultats de l'expérimentation réalisée à l'aide des prototypes orienteront l'élaboration du plan de mesure final, examiné par le CT 43/SC 3/GT 1 l'Organisation internationale de normalisation en décembre 2020 afin d'en obtenir une rétroaction et des commentaires supplémentaires.</p>					
17. Mots clés <b>l'acoustique sous-marine des navires</b>			18. Diffusion <b>Copie numérique</b>		
19. Classification de sécurité (de cette publication) <b>Non classifiée</b>	20. Classification de sécurité (de cette page) <b>Non classifiée</b>	21. Déclassification (date) <b>—</b>	22. Nombre de pages <b>65</b>	23. Prix <b>Port et manutention</b>	

# Contents

LIST OF ABBREVIATIONS AND ACRONYMS.....	IX
BACKGROUND .....	1
1.1. Acoustical terminology .....	1
1.1.1. General .....	1
1.1.2. Levels, Power Quantities, and Reference Values .....	2
1.1.3. URN Metrics.....	3
1.1.4. Sound Propagation: Concepts and Specialized Terminology .....	4
1.2. The ISO 17208-3 Process.....	4
1.2.1. ISO 17208 and ISO TC 43/SC 3/WG 1 .....	4
1.2.2. ISO 17208-1:2016.....	4
1.2.3. ISO 17208-2:2019.....	5
1.2.4. ISO 17208 Part 3 .....	5
1.2.5. Summary of ISO 17208 Measurement Protocol .....	6
1.2.6. Other Measurement Procedures.....	7
1.3. Determining Source Level from Sound Pressure Level in Shallow Water.....	7
1.4. Effects of Shallow Water on Propagation and Vessel Source Levels .....	8
1.5. Considerations for Hydrophone Geometries.....	9
1.6. Overview of the Experiment to Resolve Uncertainties in the Measurement of Underwater Noise from Ships in Shallow Water .....	12
NUMERICAL EXPERIMENTS – METHODS AND RESULTS .....	16
2.1. Research Questions.....	16
2.2. Method Overview .....	16
2.3. Propagation Models .....	17
2.3.1. MONM.....	17
2.3.2. BELLHOP.....	17
2.4. Input Parameters.....	17
2.4.1. Environment (Propagation Medium) .....	17
2.4.2. Source Model .....	18
2.4.3. Background Noise Level .....	19
2.4.4. Frequency Bands .....	20
2.4.4.1. Decidecade Bands .....	20
2.4.4.2. Centidecade Bands .....	21
2.5. Characterize Sound Field (Calculate ddec Band SPL) .....	21
2.5.1. Calculate PL in cdec Bands .....	21
2.5.2. Calculate SPL in ddec Bands .....	22
2.5.2.1. cdec Band Source Level (SL and aSL) .....	22
2.5.2.2. cdec Band Sound Pressure Level .....	23
2.5.2.3. ddec Band Sound Pressure Level .....	23
2.6. Characterize Source (Convert SPL to URN).....	23
2.6.1. Calculate RNL .....	23
2.6.2. Calculate aRNL .....	24
2.6.3. Calculate SL.....	24
2.6.4. Calculate aSL.....	24

2.6.5. Depth Average and Cylindrical Spreading: High-frequency Source Level .....	25
2.7. Results .....	25
2.7.1. Deep Water: Mud Only .....	25
2.7.1.1. PL .....	26
2.7.1.2. SPL .....	27
2.7.1.3. RNL and aRNL .....	29
2.7.1.4. SL .....	31
2.7.2. Shallow Water: Mud and Sand .....	34
2.7.2.1. PL .....	35
2.7.2.2. SPL .....	37
2.7.2.3. RNL and aRNL .....	39
2.7.2.4. SL .....	41
DISCUSSION AND CONCLUSIONS .....	44
3.1. Deep Water (200 m, mud sediment) .....	44
3.1.1. RNL and aRNL .....	44
3.1.2. SL .....	44
3.2. Shallow Water (50 m, Mud and Sand Sediments) .....	45
3.2.1. RNL and aRNL .....	45
3.2.2. SL .....	45
3.3. Preferred Processing .....	45
3.3.1. Single Hydrophone .....	46
3.3.2. Vertical Array at Five Water Depths from the Vessel .....	46
3.3.3. Horizontal Array on Seabed .....	46
3.4. Implications of a Harder Sediment in Shallow Water .....	46
LITERATURE CITED .....	47
Appendix A. Standard Frequency Bands .....	A-1
Appendix B. WG1 Bibliography .....	B-1

## Figures

Figure 1. Graph of RNL – SL versus frequency.....	5
Figure 2. Recommended geometry for making underwater radiated noise measurements.....	6
Figure 3. Sketch of multiple paths that sound travels from a ship to a recorder in shallow water. ....	8
Figure 4. Schematic of possible measurement geometries as a function of water depth assuming a closest point of approach (CPA) distance of 150 m. ....	10
Figure 5. Diagrams of three mooring designs, all deployed for long-term vessel URN measurements in Boundary Pass, BC, Canada. ....	11
Figure 6. Equivalent sound pressure levels (SPL) measured at Boundary Pass using the three different mooring design shown in Figure 5 for four different decade-wide frequency bands.....	11
Figure 8. Nominal locations to explore shallow water vessel source level recording and analysis. ....	13
Figure 9. Bathymetry at the 30 m deep site (Option 2). ....	13
Figure 10. Bathymetry at the 70 m deep site. ....	14
Figure 11. Bathymetry at the 180 m deep site. ....	14
Figure 12. Mooring designs proposed for the shallow water vessel source level experiment. (A) A three-element bottom-moored vertical array; (B) a bottom-moored volumetric array; and (C) a drifting vertical array.....	15
Figure 13. Source level spectrum used for forward modelling, based on WH02.....	18
Figure 14. Wenz ambient noise spectra, re 1 $\mu\text{Pa}^2/\text{Hz}$ . ....	19
Figure 15. Extrapolated Wenz ambient noise spectral density level (re 1 $\mu\text{Pa}^2/\text{Hz}$ ) for sea states 4 (blue) and 6 (green). ....	20
Figure 16. PL (Equation 21) re 1 $\text{m}^2$ versus range (m) and depth (m) for deep water (mud), in decibels. ....	26
Figure 17. cdec SPL (Equation 32) re 1 $\mu\text{Pa}^2$ versus range (m) and depth (m) for deep water (mud), in decibels. ....	27
Figure 18. ddec SPL (Equation 34) re 1 $\mu\text{Pa}^2$ versus range (m) and depth (m) for deep water (mud), in decibels. ....	28
Figure 19. ddec RNL (Equation 37) – aSLo (Equation 31) versus range (m) and depth (m) for deep water (mud), in decibels.....	29
Figure 20. ddec aRNL (Equation 39) – aSLo (Equation 31) versus range (m) and depth (m) for deep water (mud), in decibels.....	30
Figure 21. ddec SL (Equation 42) – SLo Equation (Equation 26) versus range (m) and depth (m) for deep water (mud), in decibels.....	31
Figure 22. ddec SL (Equation 42) – SLo (Equation 26) versus range (m) and depth (m) for deep water (mud), in decibels.....	32
Figure 23. ddec HFSL (Equation 47) – SLo (Equation 26) versus range (m) and depth (m) for deep water (mud), in decibels.....	33
Figure 24. PL (Equation 21) re 1 $\text{m}^2$ versus range (m) and depth (m) for shallow water, in decibels. ....	35
Figure 25. PL re 1 $\text{m}^2$ (dB) versus range (m) and depth (m) for deep water (mud). left: PL re 1 $\text{m}^2$ (dB). ....	36
Figure 26. cdec SPL (Equation 32) re 1 $\mu\text{Pa}^2$ versus range (m) and depth (m) for shallow water, in decibels.....	37
Figure 27. ddec SPL (Equation 34) re 1 $\mu\text{Pa}^2$ versus range (m) and depth (m) for shallow water, in decibels. ....	38
Figure 28. ddec RNL (Equation 37) – aSLo (Equation 31) versus range (m) and depth (m) for shallow water, in decibels. ....	39

Figure 29. ddec aRNL (Equation 39) – aSLo (Equation 31) versus range (m) and depth (m) for shallow water, in decibels. ....	40
Figure 30. ddec SL (Equation 42) – SLo (Equation 26) versus range (m) and depth (m) for shallow water, in decibels. ....	41
Figure 31. ddec SL (Equation 42) – SLo (Equation 26) versus range (m) and depth (m) using MONM-BELLINC, in decibels. ....	42
Figure 32. ddec HFSL (Equation 47) – SLo (Equation 26) versus range (m) and depth (m), in decibels. ....	43

## Tables

Table 1. Terms and definitions: Geometry. ....	1
Table 2. Terms and definitions: Decade and fractional decade frequency bands. ....	2
Table 3. Summary of metrics and terminology used by ISO and ANSI standards. ....	7
Table 6. Sediment types. ....	17
Table 7. Decidecade (ddec) centre frequencies. ....	20
Table 8. Centidecade (cdec) centre frequencies. ....	21
Table A-1. Decidecade frequency bands, as defined by IEC (2014), with centre frequencies between 10 Hz ( $n = -20$ ) and 100 kHz ( $n = +20$ ). ....	A-1
Table A-2. Fractional octave and fractional decade frequency bands. ....	A-2



## List of Abbreviations and Acronyms

ABS	American Bureau of Shipping
ANSI	American National Standards Institute
aRNL	adjusted RNL
ASA	Acoustical Society of America
aSL	adjusted SL
BV	Bureau Veritas
CD	Committee Draft
CPA	closest point of approach
DFO	Department of fisheries and Oceans
DIS	Draft International Standard
DNV	Det Norske Veritas Germanischer Lloyd
DSL	dipole source level
FDIS	Final Draft International Standard
HFSL	high-frequency source level
IBP	in-band power
IEC	International Electrotechnical Commission
ISO	International Organization for Standardization
MONM	Marine Operations Noise Model
NWIP	ISO New Work Item Proposal
PL	propagation loss
PSD	power spectral density
RINA	Registro Italiano Navale
RNL	radiated noise level
SC	Subcommittee
SC3	ISO TC 43/SC 3
SL	source level
SPL	sound pressure level
TC	Technical Committee
TC-IC	Transport Canada's Innovation Center
URN	underwater radiated noise
WG	Working Group
WG1	ISO TC 43/SC 3/WG 1
WH02	Wales and Heitmeyer (2002)

## Background

JASCO Applied Sciences, in collaboration with BC Ferries (BCF) and DW-ShipConsult, are executing a project sponsored by Transport Canada's Innovation Center (TC-IC) to provide results that will assist the International Standards Organization (ISO) in developing standard 17208-3 for the measurement of vessel underwater radiated noise (URN) in shallow water. Measurements in shallow water are difficult to perform because of the ways in which sound interacts with the seafloor and sea surface.

In assisting the ISO to develop standard 17208-3, this project aims to answer the question: *What combination of sensors and analysis methods yield measurements of vessel underwater sound levels in shallow water consistent with those that are known to be accurately obtained in deep water using ISO Standard 17208-1/-2?* The project has two phases: 1) development of a white paper that describes the issues associated with shallow water vessel sound level measurements and an associated measurement plan that address the identified knowledge gaps and 2) execution of the experiments and analysis of the collected measurements to address the knowledge gaps. Experimental measurements will be performed in shallow, mid, and deep water on the same ferry route.

The scope of this white paper is to analyze and illustrate the issues that complicate vessel URN measurements in shallow water, for the purpose of eliciting feedback from TC-IC and members of the ISO committee developing 17208-3 (Technical Committee (TC) 43, Subcommittee (SC) 3, Working Group (WG) 1 – TC 43/SC 3/WG 1). The white paper first provides an overview of the issues associated with making shallow water URN measurements; it then documents the results of acoustic propagation modeling numerical experiments that provide insight into where to measure, the appropriateness of different analysis techniques, and effects of sea bottom composition. The exposition concludes with recommendations for the hydrophone geometries to employ for at-sea measurements that will be performed in summer 2021.

After publication of this white paper, measurements using prototype moorings will be made in coastal waters off Halifax, NS. The input received from ISO TC 43/SC 3/WG 1 and the results of the prototype experiment will inform the development of the final measurement plan, which will be reviewed with ISO TC 43/SC 3/WG 1 in December 2020 to elicit further feedback and comments.

### 1.1. Acoustical terminology

We start by introducing the basic acoustical terminology followed in this white paper, based on ISO 18405.

#### 1.1.1. General

Geometrical parameters and fractional decade frequency bands are defined in Tables 1 and 2.

Table 1. Terms and definitions: Geometry.

Term	Definition
horizontal range ( $x$ )	horizontal distance between source and receiver
receiver depth ( $z$ )	vertical distance between sea surface and receiver
slant range: (cdec)	$r = \sqrt{x^2 + z^2}$
grazing angle ( $\theta$ )	$\theta = \text{atan}(z/x)$
seabed critical angle ( $\psi$ )	$\psi = \text{acos}(c_w/c_s)$

Table 2. Terms and definitions: Decade and fractional decade frequency bands.

Term	Definition	Notes
decade (dec)	ISO 80000-8:2020	
decidecade (ddec)	0.1 dec	One decidecade is approximately equal to one third of an octave.
Centidecade (cdec)	0.01 dec	

### 1.1.2. Levels, Power Quantities, and Reference Values

The general formula for level of a power quantity  $Q$  is:

$$L_Q = 10 \log_{10} \frac{Q}{Q_0} \text{ dB} , \quad (1)$$

relative to a reference value  $Q_0$  of the same quantity. For example, sound pressure level (SPL, symbol  $L_p$ ) is the level of the power quantity:

$$Q = \overline{p^2} , \quad (2)$$

relative to  $1 \mu\text{Pa}^2$ :

$$L_p = 10 \log_{10} \frac{\overline{p^2}}{1 \mu\text{Pa}^2} \text{ dB} . \quad (3)$$

Similarly, source level (SL, symbol  $L_S$ ) is the level of the source factor  $S$ :

$$Q = S \quad (4)$$

$$S = 10^{L_S/(10 \text{ dB})} \mu\text{Pa}^2 \cdot \text{m}^2 \quad (5)$$

relative to  $1 \mu\text{Pa}^2 \cdot \text{m}^2$ :

$$L_S = 10 \log_{10} \frac{S}{1 \mu\text{Pa}^2 \cdot \text{m}^2} \text{ dB} . \quad (6)$$

Finally, radiated noise level (RNL, symbol  $L_{RN}$ ) is the level of the power quantity:

$$Q = \overline{p^2} r^2 , \quad (7)$$

relative to the same reference quantity  $1 \mu\text{Pa}^2 \cdot \text{m}^2$ :

$$L_{RN} = 10 \log_{10} \frac{\overline{p^2} r^2}{1 \mu\text{Pa}^2 \cdot \text{m}^2} \text{ dB} . \quad (8)$$

### 1.1.3. URN Metrics

This section of text is closely based on Ainslie et al. (2020).

The process towards a shallow water URN measurement standard will require effective communication between stakeholders, which is facilitated by a harmonized and precise terminology with wide acceptance. Given that international consensus exists for ISO 18405 (2017), we follow that standard throughout this document.

For example, we adhere to ISO 18405 definitions of SL (a property of a sound source related to its radiated power), SPL (a property of the radiated sound field at a specified location), and propagation loss (PL, a transfer function; symbol  $\Delta L_{PL}$ , defined as the difference between SL and SPL). In the following, we distinguish between abbreviations such as SPL (for text) and symbols such as  $L_p$  (for equations). The definition of propagation loss (PL) as the difference between SL and SPL (ISO 18405) ensures that:

$$L_S = L_p + \Delta L_{PL} . \quad (9)$$

RNL is defined in a separate ISO standard 17208-1 (2016):

$$L_{RN} = L_p + 10 \log_{10} R^2 \text{ dB} . \quad (10)$$

Looking ahead, developing a shallow water URN measurement standard is likely to require new terminology, not yet defined by ISO 18405. For example, it might become desirable to introduce the dipole source level (DSL) (de Jong et al. 2010, Robinson et al. 2011), which is the source level of a point source and its surface-reflected image combined. The DSL is unsuitable as input to a propagation model (e.g., for sound mapping) but can be used in shallow water (as an alternative to RNL) for meaningful comparison between vessels.

Additional related terms are adjusted source level (aSL), which is closely related to DSL

$$L'_S = L_S + \Delta L_S , \quad (11)$$

and adjusted radiated noise level (aRNL), a modified form of RNL including effects such as absorption

$$L'_{RN} = L_{RN} + \Delta L_{RN} . \quad (12)$$

Computation of  $\Delta L_S$  and  $\Delta L_{RN}$  are discussed in Section 2.6. These options are discussed in Sections 2.6.2 and 2.6.4.

Finally we use *underwater radiated noise (URN)* as a generic term for SL, RNL, aSL, and aRNL.

SL, RNL, aSL, and aRNL all have the same reference value, which may be written either as  $1 \mu\text{Pa}\cdot\text{m}$  or  $1 \mu\text{Pa}^2\cdot\text{m}^2$ . There is no material difference in meaning between these two reference values. A reference value of  $1 \mu\text{Pa}^2\cdot\text{m}^2$  is used throughout this report.<sup>1</sup>

<sup>1</sup> Source level is sometimes stated with reference to “ $1 \mu\text{Pa} @ 1 \text{ m}$ ”. While there is no difference in the intended meaning between “ $1 \mu\text{Pa}\cdot\text{m}$ ” and “ $1 \mu\text{Pa} @ 1 \text{ m}$ ”, here we prefer the international standard reference value,  $1 \mu\text{Pa}\cdot\text{m}$  because source level is a far-field characteristic of the source (i.e., not at 1 m).

### 1.1.4. Sound Propagation: Concepts and Specialized Terminology

An estimate of PL is fundamental to calculating SL. Rearranging Equation 9, PL can be written:

$$\Delta L_{PL} = L_S - L_p , \quad (13)$$

and the propagation factor is

$$F = 10^{-\Delta L_{PL}/(10 \text{ dB})} \text{ m}^{-2} . \quad (14)$$

The term “spherical spreading” is used to indicate a propagation factor inversely proportional to slant range ( $r$ ) squared

$$F \propto r^{-2} . \quad (15)$$

The term “cylindrical spreading” is used to indicate a propagation factor inversely proportional to horizontal range ( $x$ )

$$F \propto x^{-1} . \quad (16)$$

For spherical spreading, PL is given by  $10\log_{10}(r^2)$  dB.

## 1.2. The ISO 17208-3 Process

This section provides an overview of the process being followed to develop the ISO 17208 standard.

### 1.2.1. ISO 17208 and ISO TC 43/SC 3/WG 1

ISO standards in underwater acoustics are developed by Sub-Committee 3 (SC 3) of ISO Technical Committee 43 (TC 43). In the following, this sub-committee is referred to as ISO TC 43/SC 3, abbreviated as “SC3”. Within SC3, the working group responsible for the development of ISO 17208 is ISO TC 43/SC 3/WG 1, abbreviated “WG1”. The convenor of WG1 is Christian Audoly.

ISO 17208 is planned as a three-part standard:

- Underwater acoustics — Quantities and procedures for description and measurement of underwater sound from ships — Part 1: Requirements for precision measurements in deep water used for comparison purposes (ISO 17208-1:2016)
- Underwater acoustics — Quantities and procedures for description and measurement of underwater sound from ships — Part 2: Determination of source levels from deep water measurements (ISO 17208-2:2019)
- Underwater acoustics — Quantities and procedures for description and measurement of underwater sound from ships — Part 3: Determination of source levels from shallow water measurements (ISO 17208-3, under development)

### 1.2.2. ISO 17208-1:2016

The development of Part 1 (ISO 17208-1) started in SC1/WG55, based on ANSI S12.64 (2009). It became the first standard produced by SC3. Work started ca. 2010 in SC 1/WG55 to develop ISO 17208. First step was the PAS (ISO 17208-1 2016).

Parts 1 and 2 are already published. Part 1 describes a procedure for measuring radiated noise level (RNL) in deep water, Equation 10. This quantity is used by Classification Societies to rank vessels according to whether they meet specified requirements for their silent classes

### 1.2.3. ISO 17208-2:2019

Part 2 (ISO 17208-2) describes a procedure for determining source level (SL) in deep water (see Equation 9). This quantity permits computation of sound pressure level at a distant location using the sonar equation from propagation loss (PL):  $SPL = SL - PL$ . The difference between RNL and SL is illustrated by Figure 1. Above ~800 Hz, the two quantities differ by 3 dB, which is related to the surface reflection that is accounted for in the source level but not in the radiated noise level.

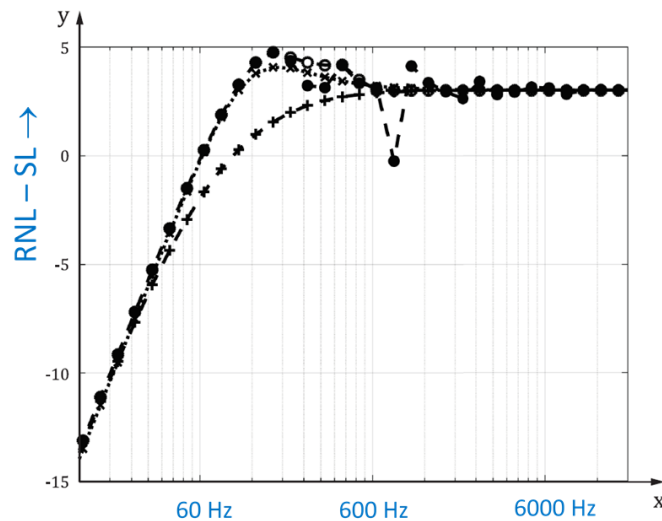


Figure 1. Graph of RNL – SL versus frequency. In the range of frequencies considered (12 Hz to 18 kHz) the difference varies between –14 dB and +5 dB for a source at a depth of 4 m.

### 1.2.4. ISO 17208 Part 3

Work on the development of Part 3 is ongoing, under the project leadership of Stephen Robinson. The material described in this white paper was presented to an online meeting of SC3 / WG 1 held on 11 August 2020.

The first step towards the development of Part 3 is the submission of a New Work Item Proposal (NWIP). The NWIP is expected to be submitted to ISO in 2020 and to include a draft measurement procedure for shallow water SL, for discussion at upcoming meetings of WG1. Subsequent steps can include:

- Committee Draft (CD, optional),
- Draft International Standard (DIS, required), and
- Final Draft International Standard (FDIS, optional).

At each WG1 meeting (typically held annually) proposals are made and discussed for different aspects of the standard. Such proposals are made by individual WG1 members. Consensus is obtained at each step, usually by incrementally improving on the initial draft, included in the NWIP. The complete process typically takes 2–4 years, corresponding to publication of ISO 17208-3 between December 2022 and December 2024 if the project starts in December 2021.

### 1.2.5. Summary of ISO 17208 Measurement Protocol

We consider the three measurement standards ANSI S12.64 (2009), ISO 17208-1 (2016), and ISO 17208-2 (2019) (Table 3). These three standards are remarkably consistent in their methodology, with ANSI S12.64 and ISO 17208-1 both measuring RNL,<sup>2</sup> and with ISO 17208-2 specifying additional processing to convert from RNL to SL. All are limited to deep water, and all consider in-band power (IBP) integrated across each frequency band, not power spectral density (PSD), averaged across the band. They all recommend the measurement geometry shown in Figure 2. The closest point of approach (CPA, distance 2 in Figure 2) between the vessel and the vertical line of hydrophones must be 100 m or the vessel length, whichever is greater. The received level is averaged over the time it takes the vessel to go from one vessel length before to one vessel length past the CPA location. The results on all three hydrophones are then averaged to obtain the URN.

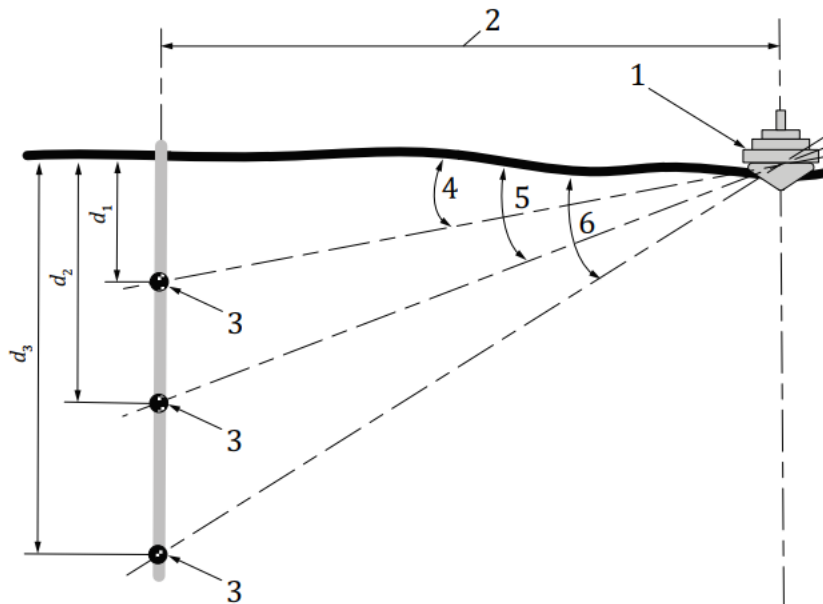


Figure 2. Recommended geometry for making underwater radiated noise measurements. (1) The vessel; (2) the closest point of approach (CPA) distance, which should be longer of 100 m or the vessel length; (3) hydrophones; and (4, 5, 6) angles to the hydrophones with target angles of 15, 30, and 45 degrees. The water depth must be greater than the CPA distance for this geometry. From ISO Standard 17208-1 (2016).

A minor difference arises in the specification of “one-third octave” frequency bands, which in early standards could mean either one third of octave (1/3 oct) or one tenth of a decade (1/10 dec), also known as a decidecade (ddec). The difference between 1/3 oct and 1/10 dec is small (about 0.08%). To make the difference explicit, ISO 18405 introduces the terms “one-third octave (base 2)” and “one-third octave (base 10)” to mean 1/3 oct and 1/10 dec, respectively (Table 3). “One-third octave (base 10)” is a synonym of decidecade. See Appendix A.

<sup>2</sup> RNL is referred to by ANSI (S12.64) as the “effective source level”.

Table 3. Summary of metrics and terminology used by ISO and ANSI standards.

Item	ANSI S12.64 (2009)	ISO 17208-1 (2016)	ISO 17208-2 (2019)	ISO/NWIP <sup>3</sup> 17208-3	Notes
Year	2009	2016	2019	2020	Estimated publication date for ISO 17208-3 is 2023
Terminology	ANSI S1.1 (R2004)	ISO 18405 (2017) <sup>4</sup>	ISO 18405	ISO 18405	
$\Delta L_{URN}$	$20 \log_{10} R$ dB	$20 \log_{10} R$ dB,	$\Delta L_{PL}$	$\Delta L_{PL}$ (to be confirmed)	
SL or RNL	RNL	RNL	SL	SL (to be confirmed)	
IBP or PSD	IBP	IBP	IBP	IBP	
Frequency bands (base <sup>5</sup> )	ANSI (S1.11 R2009) (unspecified base)	IEC 61260 (base 2 or base 10)	IEC 61260 (base 10)	IEC 61260 (base 10)	IEC 61260 last updated in 2014 ANSI S1.11 last updated in 2004

### 1.2.6. Other Measurement Procedures

Ship classification societies have developed URN measurement procedures for quiet ship certification. These are reviewed by Hannay et al. (2019) and Ainslie et al. (2020).

## 1.3. Determining Source Level from Sound Pressure Level in Shallow Water

Predicting the effects of man-made sounds on the marine ecosystem requires knowledge of amplitude and frequency content of those man-made sounds. We know that the source levels of vessels depend on vessel size, speed, draught, and trim as well as design considerations such as engine mounting, propeller design, and the flow of water over the propeller and rudders. Because of the wide range of factors that influence vessel source levels, many measurements are required to characterize the world-wide fleet. Conceptually, the SL of a vessel is easily found by measuring the SPL of the vessel as it passes a recorder and then adding the PL that accounts for the attenuation of the sound as it travelled from source to receiver, Equation 9.

For measurements made in deep water with a hydrophone far from the seabed, the direct and surface reflected paths arrive at hydrophones in the upper half of the water column with more energy than any paths interacting with the seabed. As a result, it is relatively straight-forward to account for the two paths and convert the received sound pressure level into a monopole source level without employing numerical acoustic propagation modeling. In ISO standards 17208-1, -2 and ANSI 12.64 the purpose of measuring at 15, 30, and 45° elevation (Figure 2) and averaging over repeated measurements is to smooth out the frequency dependence of the interference between the direct and reflected paths so that the URN measurement is stable.

Many entities interested in the measurement of vessel URN are located in coastal areas where the water depths are shallower than recommended in ISO 17208-2 or ANSI 12.64. In shallow water sounds interact

<sup>3</sup> The ISO working group responsible for the development of WG1. As of 3 August 2020, a NWIP was in preparation by WG1.

<sup>4</sup> ISO 17208-1 follows an advanced draft of ISO 18405. It follows the spirit of ISO 18405 but might depart in some details.

<sup>5</sup> “Base 2” and “base 10” refer to 1/3 oct and 1/10 dec, respectively.



with the seabed and multiple paths will contribute to the received sound level at a recording location. The number of paths will depend on the distance between the recorder and vessel; more paths contribute significantly to the received level at longer ranges (e.g., Figure 3). The amplitude of the seabed reflected paths depends on the incidence angles, seabed composition and bathymetric profiles. If the seabed composition, speed of sound in the water column and bathymetry are known, acoustical propagation modeling may be employed to estimate PL, and hence arrive at the source level.

The bounds on how to account for the shallow water propagation need to be defined before an approach can be considered for an international standard. For practitioners who employ acoustic propagation models, a standard could define requirements on how the geoacoustic properties were determined and how to demonstrate that the acoustic propagation model is reliable.

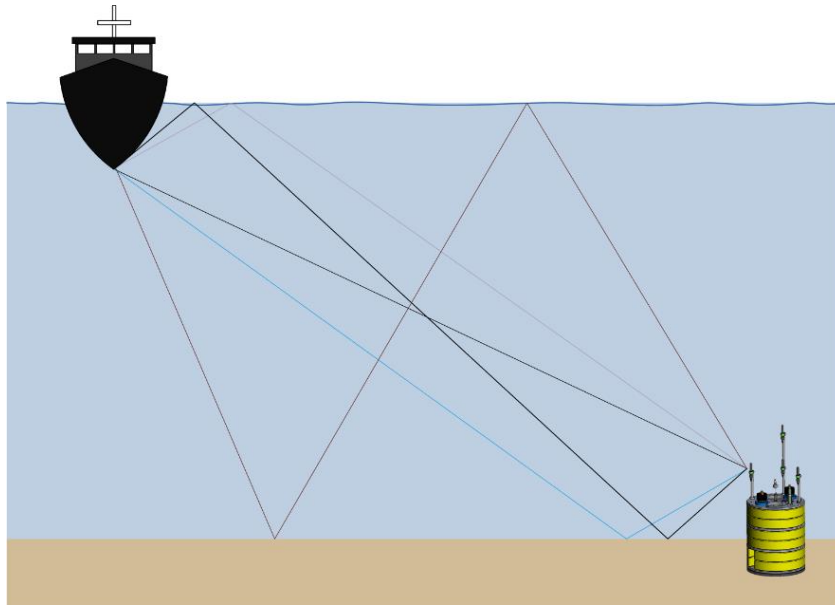


Figure 3. Sketch of multiple paths that sound travels from a ship to a recorder in shallow water.

## 1.4. Effects of Shallow Water on Propagation and Vessel Source Levels

Measurements in shallow water are not only affected by interactions of the sound with the seabed, but also by propagation and sound generation effects that are unique to this environment. First, shallow water inhibits the propagation of low frequencies in a manner that depends on the water depth and seabed composition. For most applications, 10 Hz is the minimum frequency of interest; for a typical sand seabed, a 10 Hz cut-off frequency requires a water depth of ~65 m. To avoid a situation when one single mode dominates, there needs to be at least two modes present, which in turn requires the water depth to exceed this value by a factor of three, leading to a minimum water depth of 120 m if one wanted to cover the entire frequency range of interest without entering the single mode regime. At closer ranges, this single mode criterion is less important; however, this view of propagation supports the use of 150 m depth as the division between deep and shallow water contained in ISO 17208-2.

The second effect to be considered is that resistance of water to a ship's passage increases in shallow water, which could increase propeller loading and hence noise. The International Towing Tank Committee recommends that no correction is needed if the water depth  $H$  satisfies:

$$H < \max\left(3\sqrt{BT}, 0.3 \text{ m} \left(\frac{V}{\text{m/s}}\right)^2\right), \quad (17)$$

where  $B$  is the beam of the vessel,  $T$  is the draught, and  $V$  is the vessel speed. For a vessel with a 27 m beam, 6 m draught travelling at 10 m/s (~20 knots), the minimum water depth is max (38.2, 30), which is 38.2 m.

These two constraints indicate that a minimum water depth of at least 65 m is needed to accurately measure the sound from large vessels. However, there are many places in the world where accessing water deeper than 50 m is logistically challenging. For example, much of the North Sea and Baltic Sea, both of which have heavy vessel traffic, is less than 40 m deep. Therefore, it is relevant to assess how to make measurements in these shallow areas that are comparable to the accepted deep-water methods.

## 1.5. Considerations for Hydrophone Geometries

Obtaining the received level measurements in shallow water requires careful consideration (Figure 4). The deep-water geometry is the reference whose results we would like to match to those from shallow water, but that geometry is not possible in shallow water. The guidance from ISO 17208-1 that the CPA distance be at least one vessel length remains valid, because it helps to make the approximation that the vessel is a point source more reasonable. Averaging over multiple hydrophones to smooth out propagation effects is also relevant. However, in most areas of the globe we can not deploy a bottom-mounted recording system near shipping lanes that comes closer than 25 m from the surface due to the risk of the equipment fouling a propeller. Therefore, a series of single hydrophones on the seabed could be the preferred measurement geometry to support averaging, especially in very shallow waters such as the Baltic Sea (Figure 4 B). However, the multipath propagation in shallow water (Figure 3) changes the paths much more rapidly than in deep water, which may smooth out the propagation effects and make recording at a single point acceptable, within some margin of uncertainty. A single hydrophone geometry is desirable from a cost and logistics perspective. An acoustic propagation modeling sensitivity study is required to inform the choice on where to make the shallow water measurements.

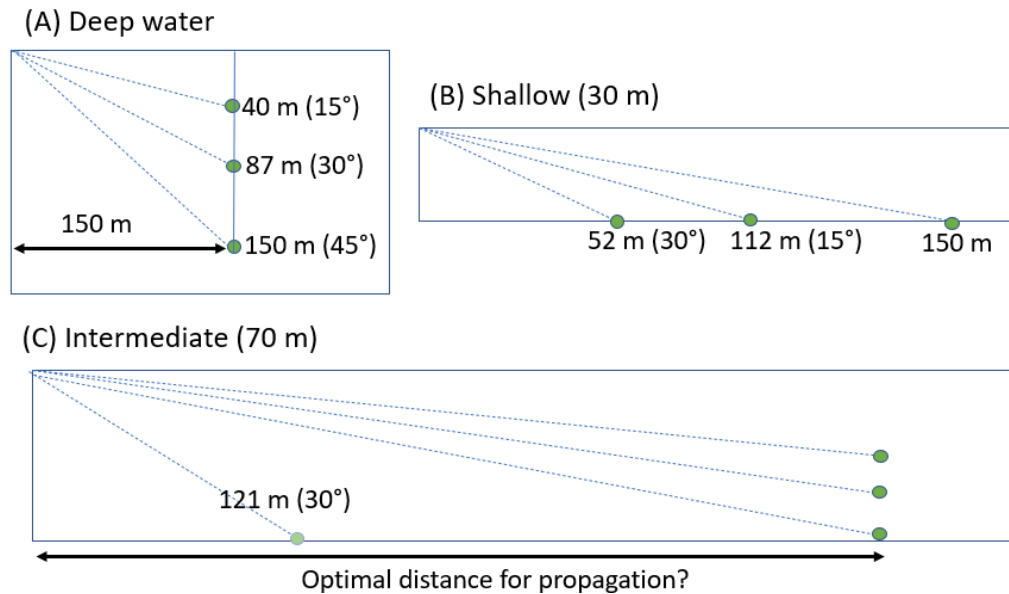


Figure 4. Schematic of possible measurement geometries as a function of water depth assuming a closest point of approach (CPA) distance of 150 m. The green dots represent hydrophones; the vessel is assumed to be in the top left corner in each configuration. (A) The deep-water geometry from ISO 17208-1/-2 and ANSI 12.64; (B) Three hydrophones spread out on the seabed for a shallow water measurement (30 m deep); and (C) A hybrid approach with a vertical array and a seabed hydrophone for intermediate depth waters.

Moored and drifting hydrophones are both appropriate for shallow water vessel URN measurements. The choice of hydrophone configuration is influenced by the nature of the program being undertaken. For measurements of a single vessel, a hydrophone system suspended over the side of a boat is the simplest and most economical approach. To establish a permanent underwater listening station, systems moored to the seabed are preferred; they could be cabled to shore or retrieved periodically and their data analyzed. Hydrophones suspended from the side of a boat often record pseudo-noise from waves slapping the side of the vessel or the hydrophones moving vertically due to wave motion, which is recorded by hydrophones due to changes in hydrostatic pressure. Bottom-moored hydrophones and vertical arrays may also record pseudo-noise due to currents flowing around the hydrophones or those currents physically moving the hydrophone and changing its depth (see Figures 5 and 6). Guidance on reducing pseudo-noise or recognizing when it is present and removing such data from vessel URN analysis ought to be considered for future standards on vessel noise measurements. Guidance is also needed on the minimum acceptable accuracy for locating hydrophones, either drifting or on the seabed, since all corrections for propagation loss (RNL and SL) are sensitive to knowing the distance between hydrophone and vessel.

### (C) Observatory

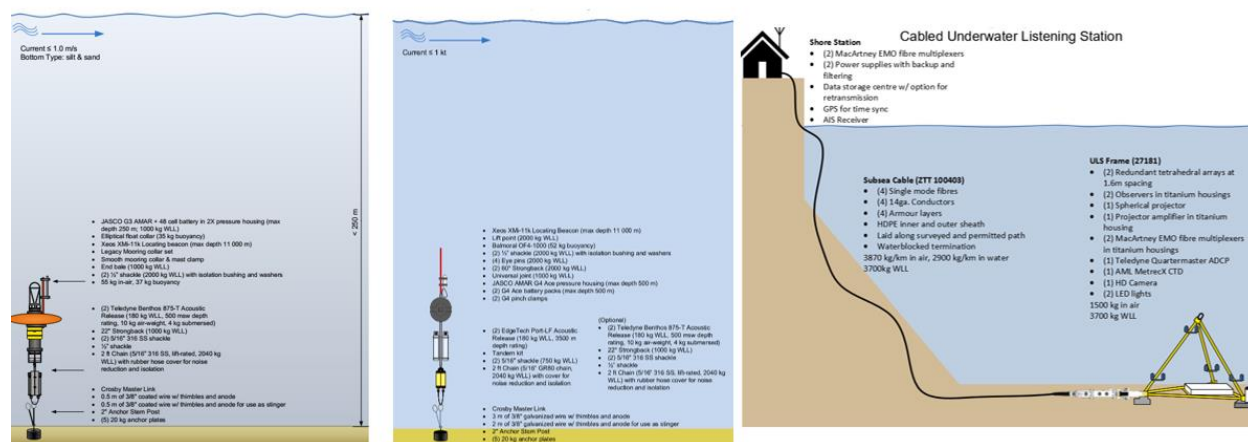


Figure 5. Diagrams of three mooring designs, all deployed for long-term vessel URN measurements in Boundary Pass, BC, Canada.

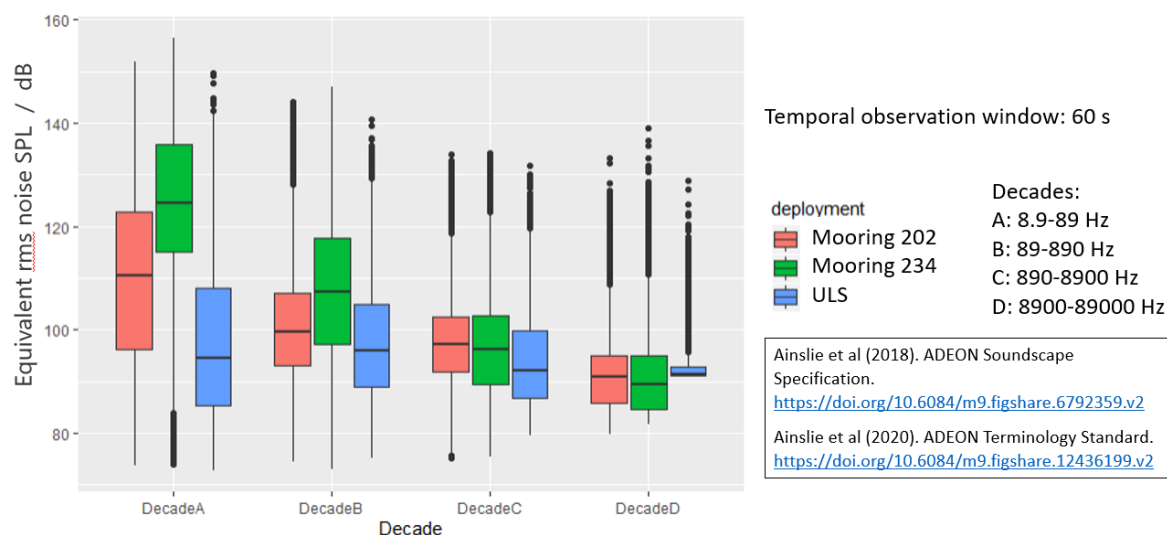


Figure 6. Equivalent sound pressure levels (SPL) measured at Boundary Pass using the three different mooring design shown in Figure 5 for four different decade-wide frequency bands. References for why those bands were employed are shown in the text box. It is expected that all three moorings received the same distribution of sound levels propagating through the water. The term 'equivalent SPL' is used because it is known that at low frequencies the measurements include pseudo-noise from currents and hydrophone movement. The seabed observatory recorded the lowest levels of pseudo-noise, followed by the mooring with the discus float; the mooring with the spherical float had the poorest performance; data from this mooring could only be used for vessel URN analysis during periods of low currents.

## 1.6. Overview of the Experiment to Resolve Uncertainties in the Measurement of Underwater Noise from Ships in Shallow Water

The sections above provide an overview of the issues associated with making reproducible measurements of vessel sound levels in shallow water. The knowledge gap that we address in this project is summarized as:

*What combination of measurement geometries and data analysis methods produce vessel URN estimates in shallow water similar to those obtained by following ISO 17208-1/-2?*

Informed by the results of the acoustic propagation modeling numerical experiments and comments from ISO TC 43/SC 3/WG 1, 10 weeks of measurements will be performed in May to July 2021. It was determined during the development of this project concept that in order to understand the relative variability of shallow water measurements compared to deep water ones, we would measure the same vessel's URN many times, in different water depths and with different measurement geometries. Our team will measure the sound radiated by ferries on a set route that pass in each direction at least six times daily.

Measurements are proposed to occur in three locations, with water depths of 30, 70, and 180 m (Figure 7). The 180 m deep site will serve as the reference deep water location for comparison to the shallow water sites. The 70 m site meets the 65 m minimum criteria (Section 1.4) for acceptable acoustic propagation at 10 Hz. The 30 m shallow water site does not meet the criteria but has a typical water depth for measurements made in the Baltic and North seas and hence is relevant for informing international standards. The bathymetry at the 30 m deep site is sloping along the ferry track but relatively flat across-track (Figure 8). The bathymetry at the 70 m site is flat all around the site (Figure 9). The 180 m deep site is in a 'bowl' that rises to 160 m depth approximately 1 km from the measurement site in all directions Figure 10.

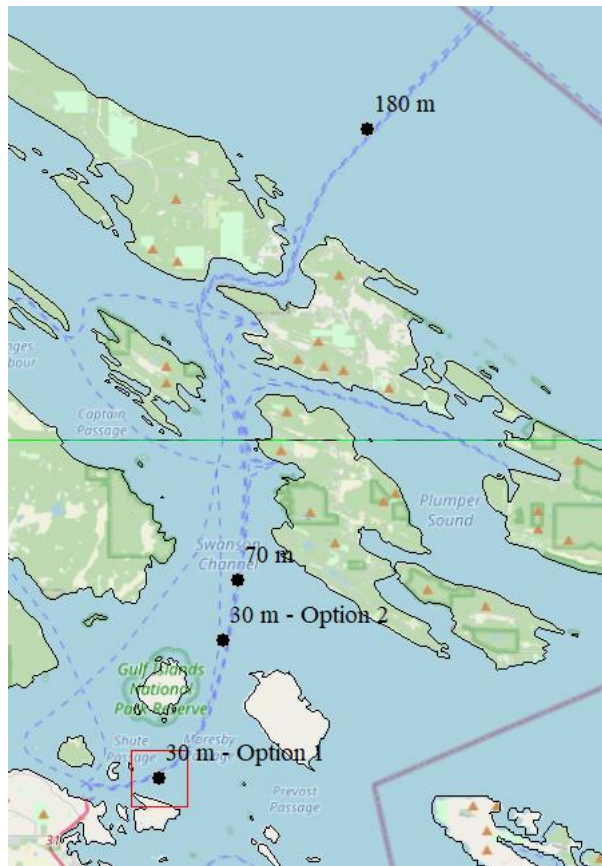


Figure 7. Nominal locations to explore shallow water vessel source level recording and analysis. The 30 m Option 1 site was originally proposed; however, the ferries are not at standard sailing speed at this location, and therefore Option 2 is currently planned.

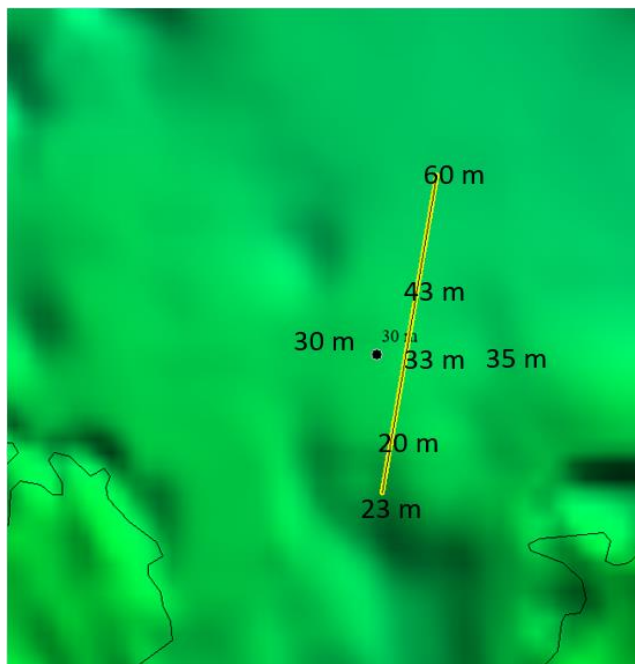


Figure 8. Bathymetry at the 30 m deep site (Option 2). A 2 km ferry track line is shown in yellow, the water depths along and around the track are annotated.

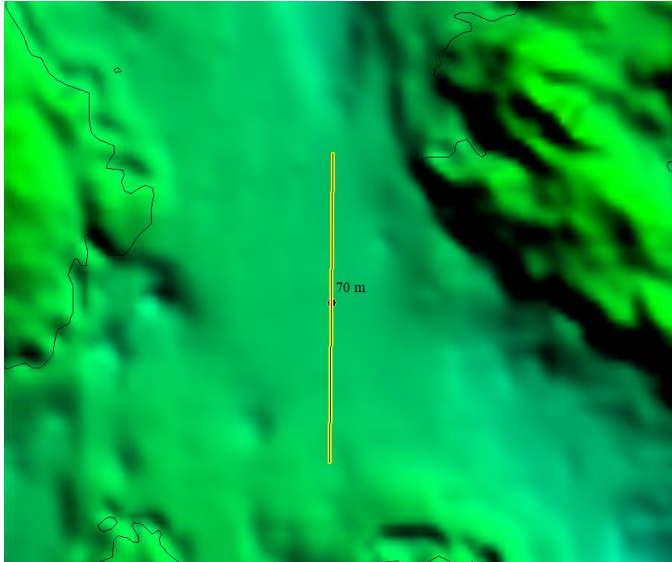


Figure 9. Bathymetry at the 70 m deep site. A 4 km ferry track line is shown in yellow; the seabed is flat  $\pm 5$  m for 1 km in each direction.

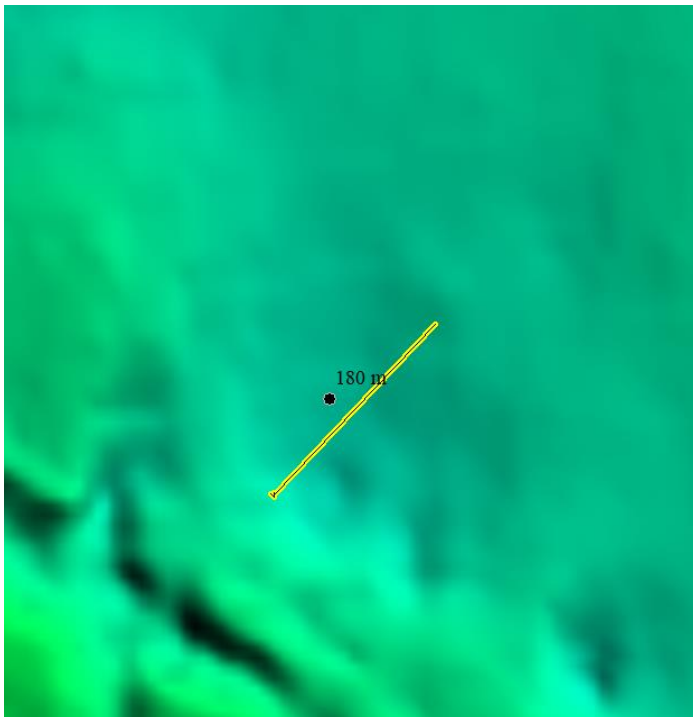


Figure 10. Bathymetry at the 180 m deep site. A 2 km ferry track line is shown in yellow; the seabed is  $\sim 160$  m deep 1 km from the measurement site in each direction.

Three hydrophone configurations are considered: a drifting vertical array, a seabed mooring, and a moored vertical array (Figure 11). The project budget provides for three vertical arrays and three bottom-mounted volumetric arrays. The proposal suggested two moorings at each site: a bottom-moored vertical array and a bottom-moored volumetric array (Figure 11 A and B). The assignment of moorings to sites will be determined through discussion with the interested members of WG1. As a minimum, a three-hydrophone vertical array will be deployed at the 180 m site to support ISO 17208-1/-2 compliant measurements.



On three occasions throughout the deployment period, we will conduct at least three measurements at each location using a drifting vertical array (Figure 11 C). The drifting measurement will be made at a nominal distance of ~200 m from the ferry at its closest point of approach. These three types of recordings will provide data compatible with all measurement configurations and data analysis methods that have been proposed for shallow water URN measurements. The volumetric arrays will allow for an analysis of small-scale variability in URN from bottom-mounted hydrophones.

An important element of this study is exploring how knowledge of the sediment properties affects the results. We will use the following three methods to estimate those properties:

1. Use the values provided from public sources, such as hydrographic survey maps, scientific literature, government reports, etc.
2. Monitor the SL at different distances from the deployment vessel as it approaches the long-term recorders and compare the SL variations with predictions from a back-propagation computer model. The back-propagation model is the same model currently used by several of the Classification Societies' Quiet Notations. The model will be run using a variety of possible bottom types. The true bottom characteristics can be determined by finding the modelled bottom characteristics that lead to the best match with measured SL at all distances from the ferry. This approach is referred to as "inversion".
3. Use a calibrated sound projector, such as the US Navy J9, to perform the inversion test described above. The J9 is a relatively low-power source so will have a limited effects zone for disturbing marine mammals. Authorization to employ the source will be obtained from the Department of fisheries and Oceans (DFO) before the experiment is conducted, and all mitigations recommended by DFO will be applied. The benefit of this test is that the SL of the source is already known, so propagation loss can be determined directly. This approach, referred to as a "Propagation Loss" study, is commonly used to calibrate acoustic ranges.

We will test how variations in the sediment properties affects the estimates of the radiated noise level and monopole source level.

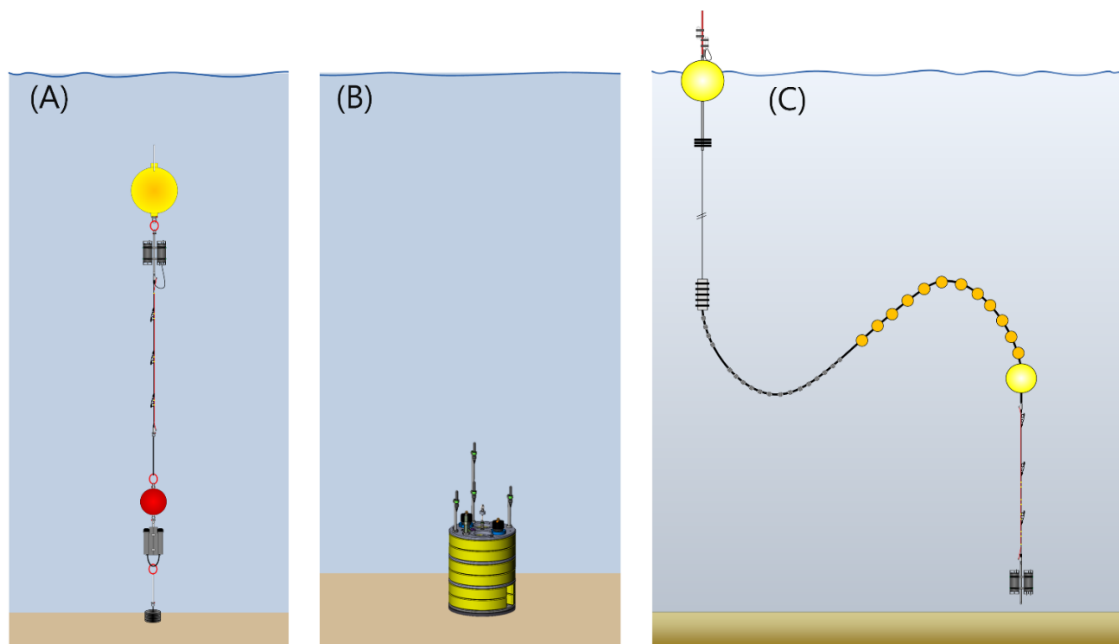


Figure 11. Mooring designs proposed for the shallow water vessel source level experiment. (A) A three-element bottom-moored vertical array; (B) a bottom-moored volumetric array; and (C) a drifting vertical array.



# Numerical experiments – Methods and Results

## 2.1. Research Questions

Research questions of interest are:

- Which of the metrics considered (SL, RNL, aSL, and aRNL) best characterizes vessel URN in shallow water?
- What shallow water geometry is best suited to characterizing vessel URN? (i.e., which geometry most closely reproduces deep water value measured using ISO 17208-1 or -2)?

## 2.2. Method Overview

The overall approach has two steps. First, we predict the sound field generated by a source ship using centidecade (cdec) bands, sum the cdec bands to synthesize decade (ddec) band quantities; the ddec band levels become our 'truth' received levels. Second, we see how well we can estimate the original source properties from the synthesized ddec band quantities by considering propagation only at the ddec centre frequencies. The difference between the two values is an anomaly we seek to minimize by optimizing the configuration of data collection hydrophones and choice of URN metric, and by selecting seabeds with desirable propagation properties.

Specifically, we carry out the following steps:

- Verify propagation models used for estimating properties of individual cdec bands and of ddec band centre frequencies
- Estimate source properties as a function of frequency from 10 Hz to 100 kHz. The main metrics considered are SL and RNL. Also considered are aSL and aRNL (Ainslie et al. 2020).
- Assess the suitability of these source properties at selected frequencies (30 Hz, 300 Hz, 3 kHz, and 30 kHz). Most of the sound radiated by surface vessels is at frequencies below 1 kHz, so it is tempting to focus on 30 and 300 Hz only. We avoid this temptation because of the need to consider animals' hearing sensitivity. For example, if an animal's hearing range is limited to frequencies above 10 kHz, the most relevant frequency for that animal would be 30 kHz.
- Compare the inferred URN values (SL, RNL, aSL, and aRNL) with expected values of these metrics by plotting in the form of the difference between the inferred value and the expected value.

## 2.3. Propagation Models

We used a parabolic equation model (MONM) and a raytrace model (BELLHOP). In deep water (200 m), results from MONM and BELLHOP are compared. In shallow water (50 m), mainly MONM was used, with occasional comparisons with BELLHOP where a specific need arises.

### 2.3.1. MONM

MONM computes acoustic propagation via a wide-angle parabolic equation solution to the acoustic wave equation (Collins 1993) based on a version of the U.S. Naval Research Laboratory's Range-dependent Acoustic Model (RAM), which has been modified to account for an elastic seabed (Zhang and Tindle 1995). The parabolic equation method has been extensively benchmarked and is widely employed in the underwater acoustics community (Collins et al. 1996). MONM accounts for the additional reflection loss at the seabed due to partial conversion of incident compressional waves to shear waves at the seabed and sub-bottom interfaces, and it includes wave attenuations in all layers. MONM-RAM incorporates the following site-specific environmental properties: a modeled area bathymetric grid, underwater sound speed as a function of depth, and a geoacoustic profile based on the overall stratified composition of the seafloor.

### 2.3.2. BELLHOP

BELLHOP employs Gaussian beam acoustic ray-trace model (Porter and Liu 1994). This version of MONM accounts for sound attenuation due to energy absorption through ion relaxation and viscosity of water in addition to acoustic attenuation due to reflection at the medium boundaries and internal layers (Fisher and Simmons 1977). The former type of sound attenuation is significant for frequencies higher than 5 kHz and cannot be neglected without noticeably affecting the model results. BELLHOP incorporates the following site-specific environmental properties: a modeled area bathymetric grid, underwater sound speed as a function of depth, average temperature and salinity in the water column for calculating the sound attenuation due to energy absorption, and geoacoustic properties of the surficial sediments.

## 2.4. Input Parameters

### 2.4.1. Environment (Propagation Medium)

Two water depths are considered, 200 m ("deep") and 50 m ("shallow"). In deep water, a very fine silt "mud" seabed was modeled. In shallow water, results for a mud sediment are compared with very fine sand ("sand", Table 4).

Table 4. Sediment types. Based on Ainslie (2010).

Bottom type	$\rho$ / (kg·m <sup>-3</sup> )	$c_p$ / (m·s <sup>-1</sup> )	$\beta_p$ / (dB·λ <sup>-1</sup> )	$c_s$ / (m·s <sup>-1</sup> )	$\beta_s$ / (dB·λ <sup>-1</sup> )
Very fine silt	1439	1508.1	0.11	0	0
Very fine sand	2086	1679.7	0.88	0	0

The sea surface is treated as a smooth perfectly reflecting boundary. This approach neglects effects of scattering and absorption by near-surface bubbles and scattering by the sea surface. We compensate for neglecting these high-frequency loss mechanisms by using an artificially high value for seawater absorption. Specifically, a temperature of 22 °C and practical salinity of 40 are chosen. For acidity, we use pH = 8 (NBS scale), although the effect of acidity is small. The absorption coefficient of François and Garrison (1982) was used.

Other seawater properties assumed are sound speed and density of 1500 m/s and 1000 kg/m<sup>3</sup>, respectively

## 2.4.2. Source Model

The source level used to simulate the vessel sound field is based on Wales and Heitmeyer (2002), henceforth abbreviated WH02. The WH02 source spectral density level is (Figure 12 left):

$$L_{WH02}(f) = 230.0 \text{ dB} - 10 \log_{10}(\hat{f}^{3.594}) \text{ dB} + 10 \log_{10} \left[ \left( 1 + \left( \frac{\hat{f}}{340} \right)^2 \right)^{0.917} \right] \text{ dB}, \quad (18)$$

where  $\hat{f}$  is the numerical value of the acoustic frequency  $f$ , in hertz, i.e.,  $\hat{f} = f / (1 \text{ Hz})$ . Equation 18 is valid in the range  $30 \text{ Hz} < f < 1200 \text{ Hz}$ . It is extrapolated outside this range using Ainslie et al. (2018):

$$L_{S,f}(f) = \begin{cases} L_{WH02}(f) & f \geq 30 \text{ Hz} \\ L_{WH02}(30 \text{ Hz}) & f < 30 \text{ Hz} \end{cases} \quad (19)$$

The source model is completed by specifying a source depth of  $d = 3.4 \text{ m}$  (Ainslie et al. 2018). Adjusted source level (aSL) (Figure 12 right) is the source level of a dipole comprising the source and its surface-reflected image, evaluated at an angle of  $30^\circ$  from the horizontal (see Section 2.6.4).

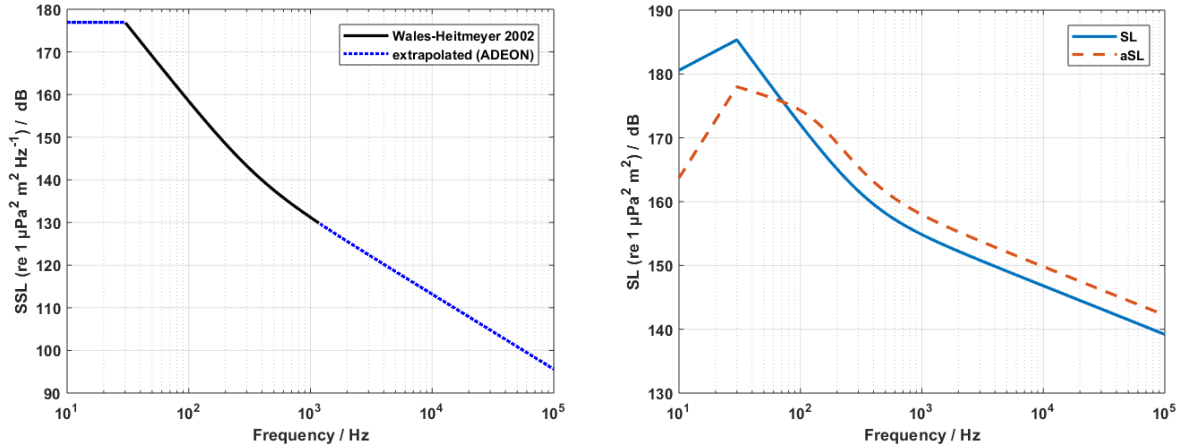


Figure 12. Source level spectrum used for forward modelling, based on WH02. Left: SSL re  $1 \mu\text{Pa}^2 \text{ m}^2/\text{Hz}$  (dB); right: ddec band source level (SL) re  $1 \mu\text{Pa}^2 \text{ m}^2$  (blue line) and adjusted source level (aSL) re  $1 \mu\text{Pa}^2 \text{ m}^2$  (dashed red).

### 2.4.3. Background Noise Level

Background noise based on Wenz sea state 4 (Figure 13) is included in the calculation of ddec band SPL. In order to allow for other sources of noise (system noise and shipping noise), the noise spectral density level was artificially held flat (Figure 14) at both high frequency (above 24 kHz) and low frequency (below 150 Hz). Sea state 6 has been used in other studies as the environmental noise floor and is included in Figure 14 for reference.

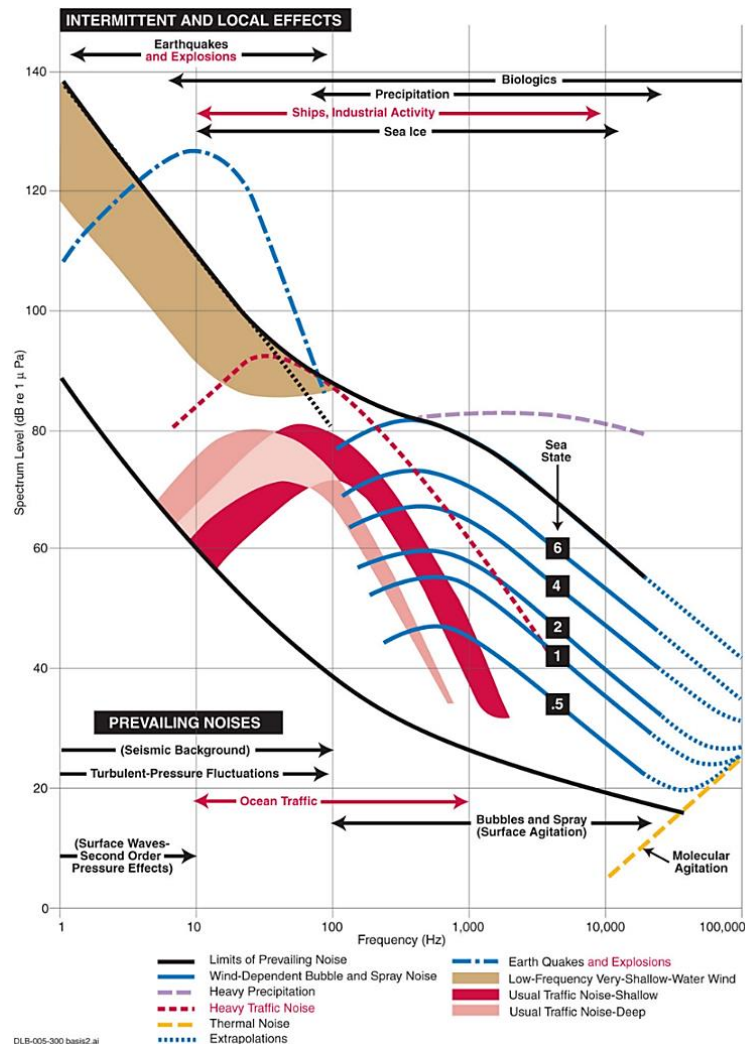


Figure 13. Wenz ambient noise spectra, re 1  $\mu\text{Pa}^2/\text{Hz}$ . ((Miksis-Olds et al. 2013) adapted from (Wenz 1962)).

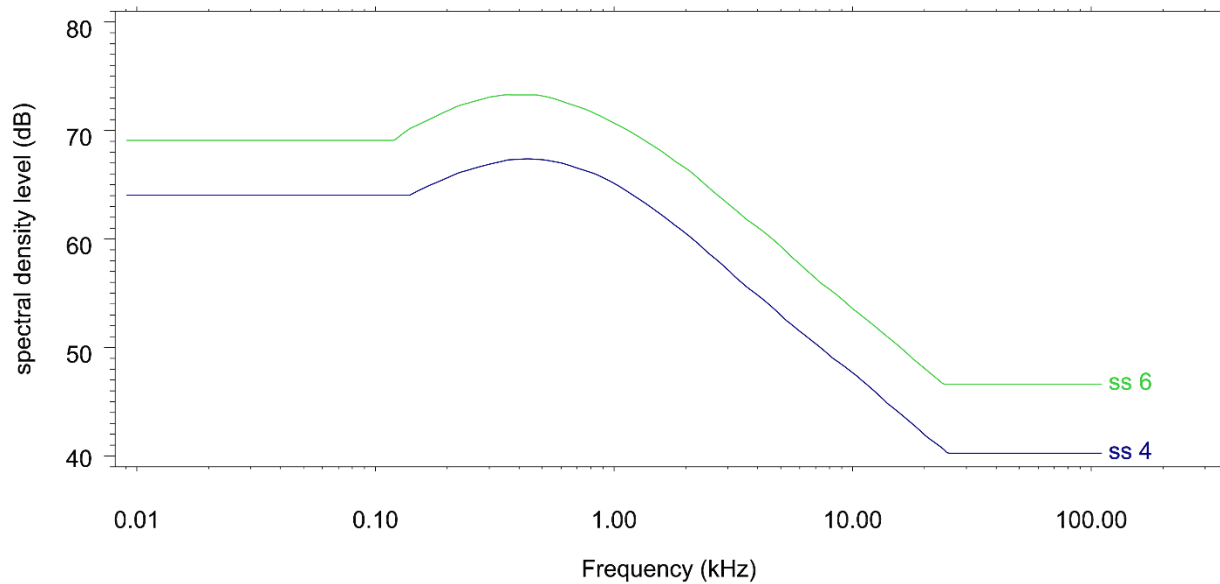


Figure 14. Extrapolated Wenz ambient noise spectral density level (re  $1 \mu\text{Pa}^2/\text{Hz}$ ) for sea states 4 (blue) and 6 (green).

## 2.4.4. Frequency Bands

### 2.4.4.1. Decidecade Bands

The frequency range 10 Hz to 100 kHz is considered using 41 decidecade bands, with centre frequencies corresponding to index  $m = -20:1:+20$ , in

$$f_c = 10^{0.1m} \cdot (1 \text{ kHz}), \quad (20)$$

which is compliant with IEC (2014). Specifically, the first and last few decidecade centre frequencies are listed in Table 5. See Appendix A for a complete list. The total frequency range covered by these 41 bands is 8.9 Hz to 112 kHz.

Table 5. Decidecade (ddec) centre frequencies. Frequencies are rounded to 3 significant figures.

decidedade index ( <i>m</i> )	<i>f<sub>c</sub></i> / Hz
-20	10.0
-19	12.6
-18	15.8
..	
+19	79 400
+20	100 000

#### 2.4.4.2. Centidecade Bands

Each decade band is sub-divided into 10 centidecade bands. The corresponding cdec centre frequencies are obtained by substitution of index  $m = -20.45:0.1:+20.45$  in Equation 20. The first and last few centidecade centre frequencies are listed in Table 6.

Table 6. Centidecade (cdec) centre frequencies. Frequencies are rounded to 3 significant figures.

decidedade index ( $m$ )	fc / Hz
-20.45	9.02
-20.35	9.23
-20.25	9.44
...	
+20.35	108 000
+20.45	111 000

## 2.5. Characterize Sound Field (Calculate ddec Band SPL)

The ddec band SPL is computed using the following steps:

1. Calculate PL from source to receiver in 410 cdec bands (10 Hz to 100 kHz);
2. Calculate vessel contribution to cdec band SPL;
3. Add noise contribution to cdec band SPL; and
4. Add ten successive cdec bands from ddec band SPL.

### 2.5.1. Calculate PL in cdec Bands

PL is calculated at cdec centre frequencies using:

$$\Delta L_{PL,m,\alpha}(x, z) = \Delta L_{PL,m,0}(x, z) + \alpha_m r_-(x, z), \quad (21)$$

where  $z$  and  $x$  are the depth and horizontal range of the receiver,  $\Delta L_{PL,m,0}$  is the propagation loss without absorption, and  $\alpha_m$  is the absorption coefficient at the cdec centre frequency,  $r_-$  is the slant range

$$r_-(x, z) = (x^2 + (z - d)^2)^{1/2} \quad (22)$$

and  $d$  is the source depth.

Use of Equation 21 ensures that absorption is correctly estimated for the direct path in each cdec band, accepting that the contribution from other (typically weaker) multipaths might be overestimated by underestimating the associated absorption for those paths.

## 2.5.2. Calculate SPL in ddec Bands

### 2.5.2.1. cdec Band Source Level (SL and aSL)

The cdec band source level is approximated by:

$$L_{S,m} = L_{S,f} + 10 \log_{10} \frac{\delta f_m}{1 \text{ Hz}} \text{ dB} , \quad (23)$$

where  $\delta f_m$  is the bandwidth of the band and is given by:

$$\delta f_m = (10^{+0.005} - 10^{-0.005}) f_{c,m} , \quad (24)$$

i.e.,

$$\delta f_m \approx 0.023026 f_{c,m} . \quad (25)$$

Using the upper case subscript  $M$  to indicate a ddec band (lower case  $m$  indicates a cdec band), the ddec WH02 SL is then obtained by power addition:

$$L_{S,M}(x, z) = 10 \log_{10} \sum_{n=0}^9 10^{L_{S,m(n)}/(10 \text{ dB})} \text{ dB} , \quad (26)$$

where

$$m(n) = M - 0.45 + 0.1n . \quad (27)$$

Adjusted source level (symbol  $L'_S$ ) is calculated from cdec SL ( $L_S$ ), from Equation 23 (Ainslie et al. 2020):

$$L'_{S,m} = L_{S,m} + 10 \log_{10} \overline{\sigma}_m \text{ dB} , \quad (28)$$

where  $\overline{\sigma}_m$  is (ISO 17208-2):

$$\overline{\sigma}_m \approx \frac{14(k_m d)^2 + 2(k_m d)^4}{14 + 2(k_m d)^2 + (k_m d)^4} , \quad (29)$$

where  $d$  is the source depth and  $k_m$  is the wave number at each frequency given by:

$$k_m = \frac{2 \pi f_m}{c} . \quad (30)$$

The ddec band aSL is obtained by adding the contributions from ten successive cdec bands (again using power addition):

$$L'_{S,M}(x, z) = 10 \log_{10} \sum_{n=0}^9 10^{L'_{S,m(n)}/(10 \text{ dB})} \text{ dB} . \quad (31)$$

### 2.5.2.2. cdec Band Sound Pressure Level

The contribution to SPL from the vessel at each point at a horizontal distance  $x$  and depth  $z$  from the source is:

$$L_{p,m}(x, z) = L_{S,m} - \Delta L_{PL,m,\alpha}(x, z). \quad (32)$$

The contribution to the cdec SPL from the background noise sets a SPL noise floor as a function of frequency that is approximated by:

$$L_{n,m} = L_{n,f} + 10 \log_{10} \frac{\delta f_m}{1 \text{ Hz}} \text{ dB}, \quad (33)$$

where  $L_{n,f}$  is the noise spectral density for sea state 4, as represented by Figure 14.

### 2.5.2.3. ddec Band Sound Pressure Level

The ddec band SPL is obtained by power addition over ten successive cdec bands:

$$L_{p,M}(x, z) = 10 \log_{10} \sum_{n=0}^9 \left( 10^{L_{p,m(n)}(x,z)/(10 \text{ dB})} + 10^{L_{n,m(n)}/(10 \text{ dB})} \right) \text{ dB}. \quad (34)$$

## 2.6. Characterize Source (Convert SPL to URN)

The main source metrics considered are RNL (Section 2.6.1) and SL (Section 2.6.3), and modifications to these aRNL (Section 2.6.2) and aSL (Section 2.6.4). A high-frequency approximation to SL is also considered (Section 2.6.5).

### 2.6.1. Calculate RNL

RNL is calculated first as:

$$L_{RN,\theta_1}(x, z) = L_{p,M}(x, z) + 10 \log_{10} \frac{x^2 + z^2}{1 \text{ m}^2} \text{ dB}. \quad (35)$$

The angle  $\theta_1$  is determined by the measurement geometry

$$\theta_1 = \arcsin \frac{z}{(x^2 + z^2)^{1/2}}. \quad (36)$$

For a given vessel, RNL varies with the value of  $\theta_1$ , and this angle dependence needs to be removed to ensure a like-with-like comparison. We therefore convert RNL to a common angle of  $30^\circ$ , chosen for compatibility with ISO 17208

$$L_{RN,30} = L_{RN,\theta_1} + 10 \log_{10} \frac{\sigma(\pi/6)}{\sigma(\theta_1)} \text{ dB}, \quad (37)$$

where the value of  $\sigma(\theta)$  (the ratio of dipole source factor to monopole source factor) is (combining equations 8.188 and 8.190 from Ainslie (2010); see also de Jong et al. (2010) and Ainslie et al. (2020))

$$\sigma(\theta) \approx \left( \frac{1}{2} + \frac{c^2}{(4\pi d f_M \sin \theta)^2} \right)^{-1}. \quad (38)$$



### 2.6.2. Calculate aRNL

To calculate aRNL, we use (Ainslie et al. 2020):

$$L'_{RN} = L_{RN,30} + \Delta L_H + \Delta L_\alpha \quad (39)$$

where

$$\Delta L_\alpha = \alpha(x^2 + z^2)^{1/2} \quad (40)$$

and

$$\Delta L_H = -10 \log_{10} \left( 1 + \frac{\psi(x^2 + z^2)^{1/2}}{H} \right) \text{ dB} , \quad (41)$$

where  $\psi$  is the critical angle and  $H$  is the water depth.

### 2.6.3. Calculate SL

The ddec SL is estimated using:

$$L_{S,M}(x, z) = L_{p,M}(x, z) + \Delta L_{PL}(x, z) , \quad (42)$$

where  $\Delta L_{PL}$  is PL at the ddec centre frequency and  $L_{p,M}$  is given by Equation 34.

### 2.6.4. Calculate aSL

Adjusted source level (abbreviation aSL, symbol  $L'_s$ ) is calculated from ddec SL ( $L_s$ ) using the same method as for Equation 28, except that here it is applied to ddec bands:

$$L'_{S,M}(x, z) = L_{S,M}(x, z) + 10 \log_{10} \overline{\sigma}_M \text{ dB} , \quad (43)$$

where  $\overline{\sigma}_M$  is (following Ainslie et al. 2020):

$$\overline{\sigma}_M \approx \frac{14(k_M d)^2 + 2(k_M d)^4}{14 + 2(k_M d)^2 + (k_M d)^4} , \quad (44)$$

where  $d$  is the source depth and

$$k_M = \frac{2 \pi f_M}{c} . \quad (45)$$

The aSL is the DSL evaluated at a grazing angle of 30°.

## 2.6.5. Depth Average and Cylindrical Spreading: High-frequency Source Level

The level of the depth-averaged mean-square sound pressure is:

$$L_{p,M,av}(x) = 10 \log_{10} \frac{1}{N} \sum_{n_H}^{n_{H-h}} 10^{L_{p,M}(x,z_n)/(10 \text{ dB})} \text{ dB} , \quad (46)$$

where  $H$  is the water depth,  $h$  is the height of the receiver from the seabed and the average runs over depth  $z_n$  from  $H - h$  to  $H$ , where  $h$  is the height above the seabed. The sum is carried out over a depth grid with vertical spacing 1/3 m.

The ddec band high-frequency source level (HFSL) is

$$L_{S,M,HF}(x) = L_{p,M,av}(x) + 10 \log_{10} \frac{F_{CS}(x)^{-1}}{1 \text{ m}^2} \text{ dB} , \quad (47)$$

where  $F_{CS}$  is a depth-averaged high-frequency propagation factor for cylindrical spreading (Ainslie 2010, Ainslie et al. 2014):

$$F_{CS}(x) = \frac{2\psi}{xH} \exp(-2 \alpha x) , \quad (48)$$

where  $\psi$  is the critical angle of the seabed.

## 2.7. Results

URN metrics are simulated in the frequency range: 10 Hz to 100 kHz (index  $M = -20:1:+20$ ). This white paper includes results for 30 Hz, 300 Hz, 3 kHz, and 30 kHz.

### 2.7.1. Deep Water: Mud Only

Deep water results are presented for MONM and BELLHOP, for a mud sediment. Except where stated otherwise, BELLHOP is run in coherent mode.

PL is calculated in cdec bands (Section 2.7.1.1, Figure 15). SPL is calculated in cdec and ddec bands (Section 2.7.1.2, Figures 16 and 17). The ddec band SPL includes a contribution from background noise (sea state 4, Figure 14) and is averaged in range in a way that simulates a vessel transit, for a 30° data window.

Multiple URN metrics are calculated from ddec band SPL in ddec bands (Sections 2.7.1.3 and 2.7.1.4). For each URN metric calculated using the methods described in Section 2.6, the calculated value (URN) is compared with the expected value (URN<sub>o</sub>) of that metric and plotted (Figures 18–22) in the form of the difference between the calculated and expected value (dURN = URN – URN<sub>o</sub>). These graphs show the difference dURN plotted versus horizontal range  $x$  and depth  $z$ . White indicates dURN = 0, while blue and red indicate dURN > 0 and dURN < 0, respectively; the deeper the colour the larger the magnitude of dURN. Results for aSL are omitted because the error in aSL is the same as the error in SL.

### 2.7.1.1. PL

PL is needed for both the forward calculation of SPL in cdec bands (Equation 32) and the inverse calculation of SL in ddec bands (Equation 42). The pattern of interference lobes changes with frequency, with implications for optimal choice of processing.

Figure 15 shows PL versus range and depth for MONM (left) and BELLHOP (right), for frequencies (increasing top to bottom) 30 Hz, 300 Hz, 3 kHz, and 30 kHz. Agreement between the two models, and hence the confidence in both, increases with increasing frequency.

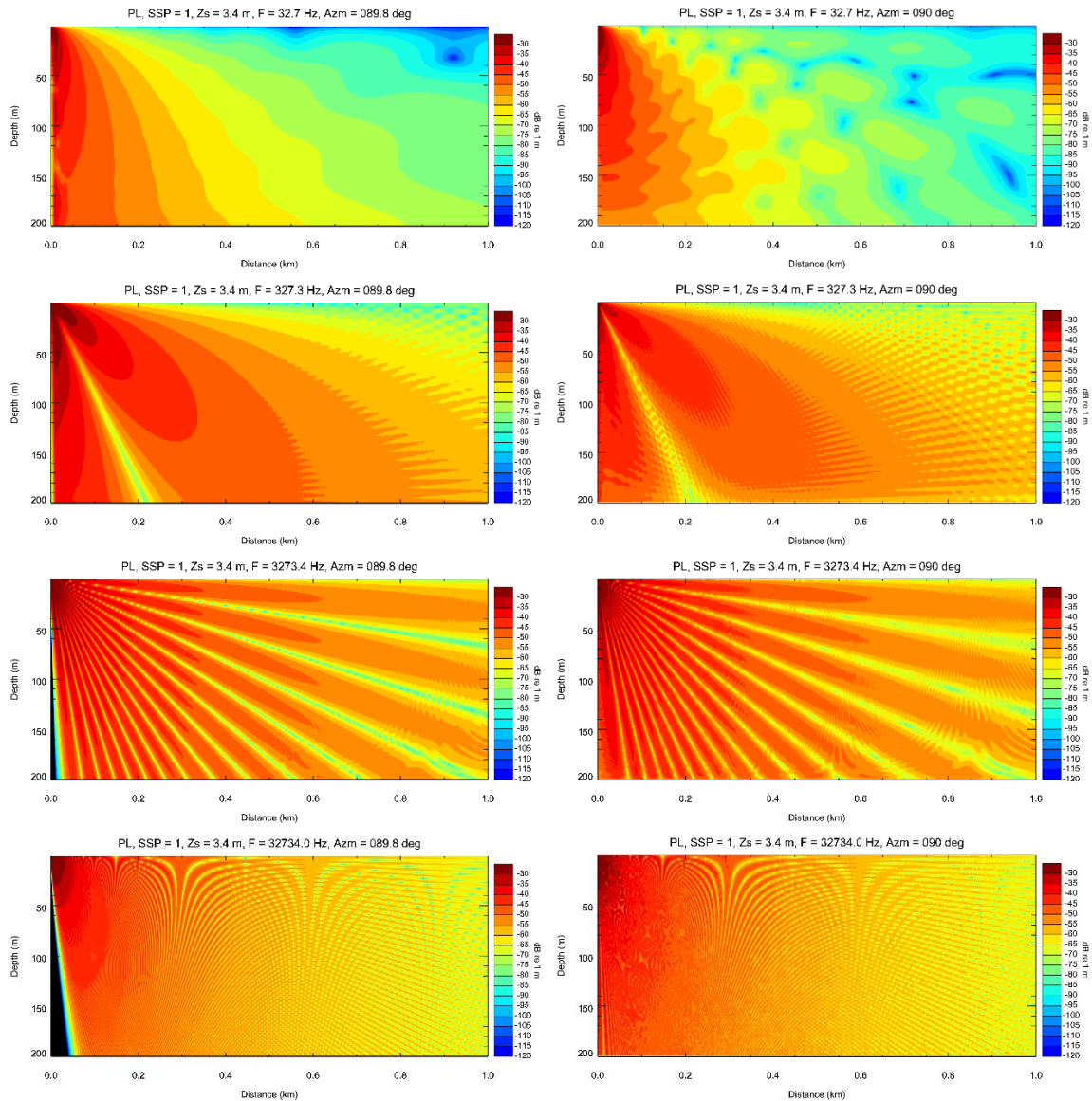


Figure 15. PL (Equation 21) re  $1 \text{ m}^2$  versus range (m) and depth (m) for deep water (mud), in decibels. Left: MONM; right: BELLHOP.

### 2.7.1.2. SPL

Figure 16 shows cdec SPL versus range and depth for MONM (left) and BELLHOP (right), for frequencies (increasing top to bottom) 30 Hz, 300 Hz, 3 kHz, and 30 kHz. The cdec SPL is calculated directly as SL minus PL, hence the similarity with PL from Figure 15.

Decade (ddec) SPL (Figure 17) is calculated by summing over ten cdec bands, adding noise and averaging over range. Figure 17 is therefore similar to Figure 16 but with smoother contours.

As in the case of PL, agreement between the two models increases with increasing frequency.

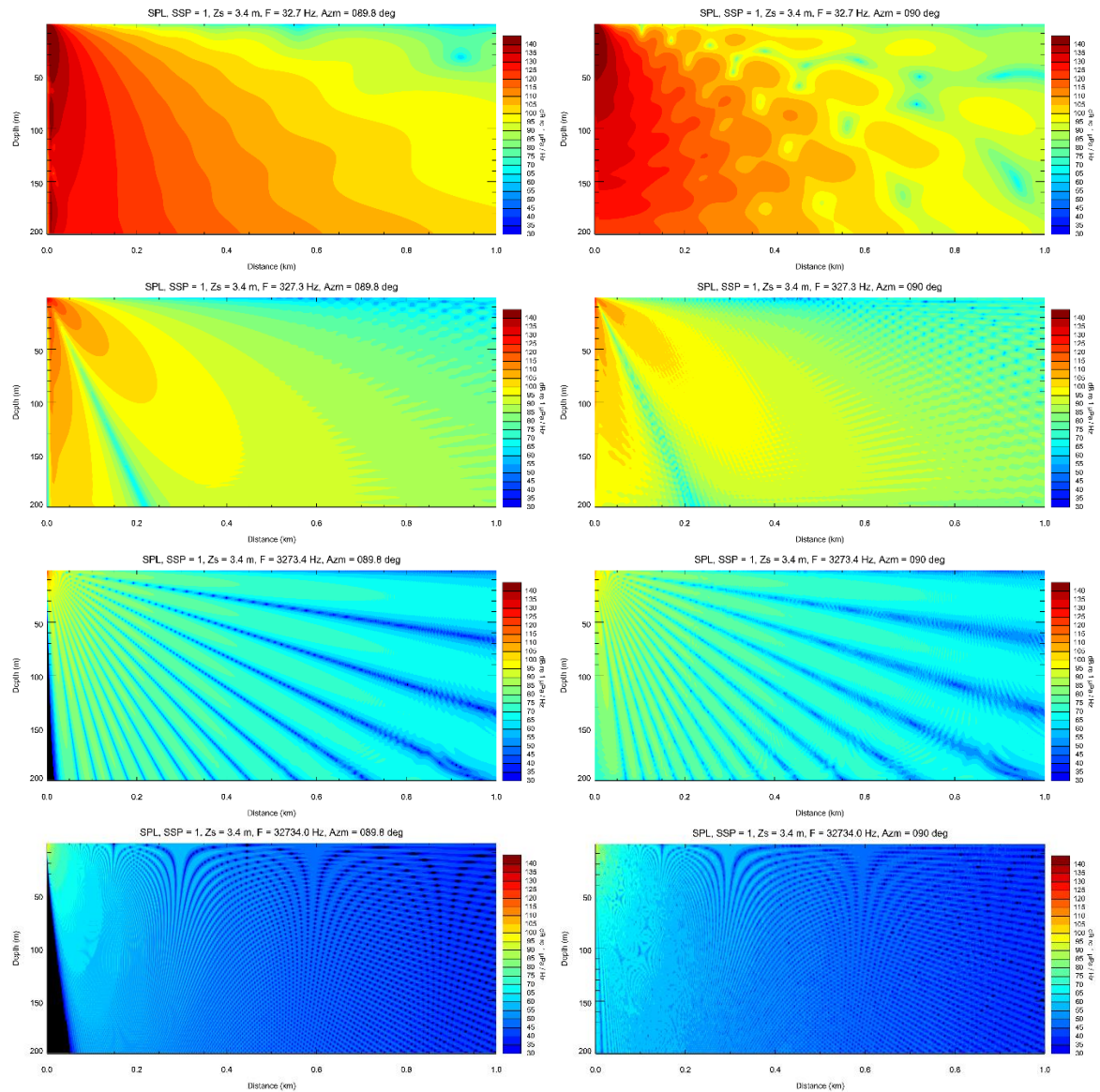


Figure 16. cdec SPL (Equation 32) re  $1 \mu\text{Pa}^2$  versus range (m) and depth (m) for deep water (mud), in decibels. Left: MONM; right: BELLHOP.

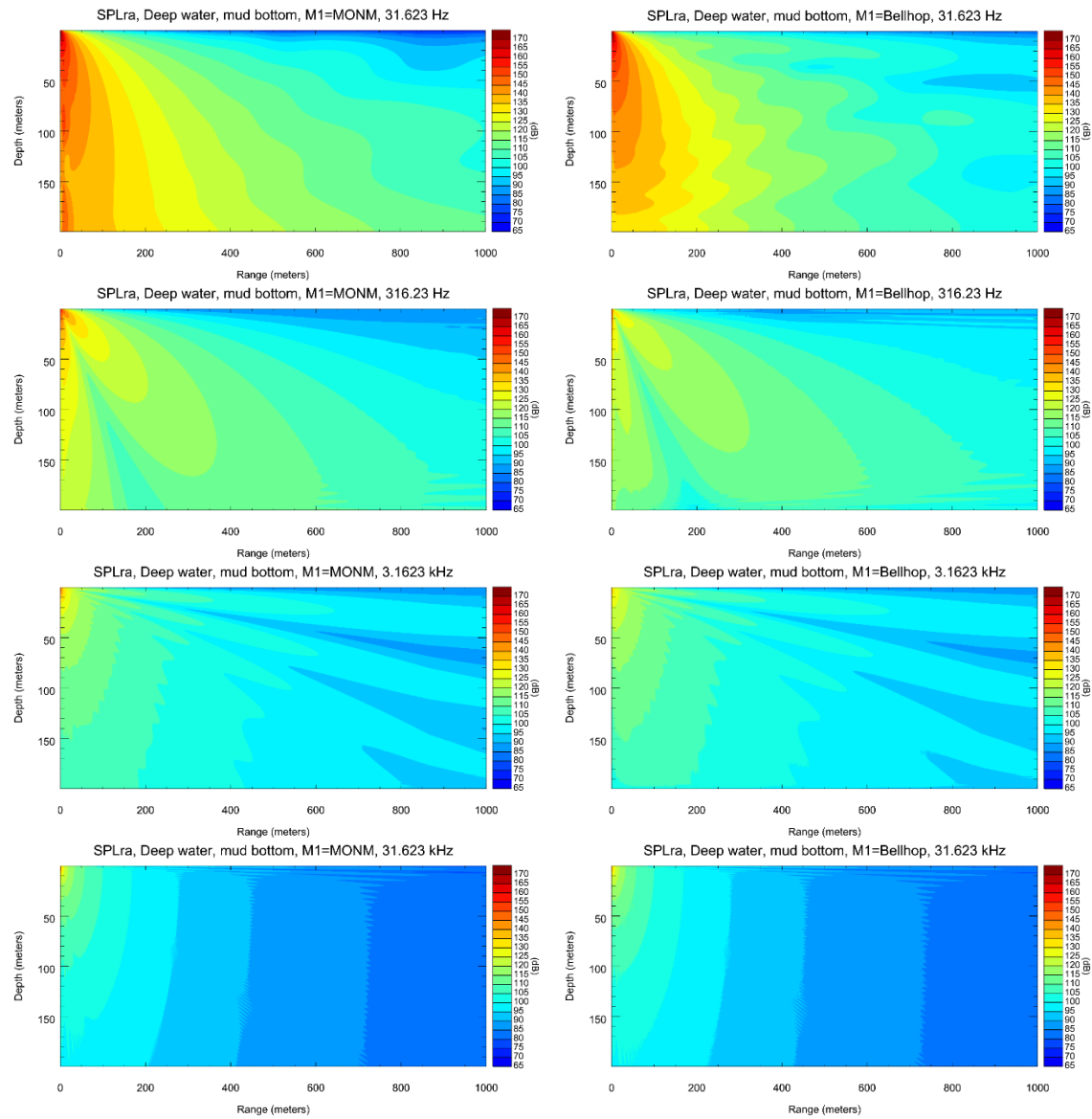


Figure 17. ddec SPL (Equation 34) re  $1 \mu\text{Pa}^2$  versus range (m) and depth (m) for deep water (mud), in decibels. Left: MONM; right: BELLHOP. Decidecade (ddec) SPL includes contributions from both signal (sound from the vessel) and background noise, and is averaged over range to represent a  $30^\circ$  data window for a passing vessel.



### 2.7.1.3. RNL and aRNL

RNL (Figure 18) is compared with aSLo (Equation 31). Blue and red indicate regions where RNL is over- and under-estimated, respectively, relative to aSLo. The procedure is effective at 3 kHz and above. Interference effects at 300 Hz and below suggests a possible need for improved processing at these frequencies. Apart from a small absorption correction at 30 kHz, the aRNL in deep water (Figure 19) is approximately equal to RNL from Figure 18.

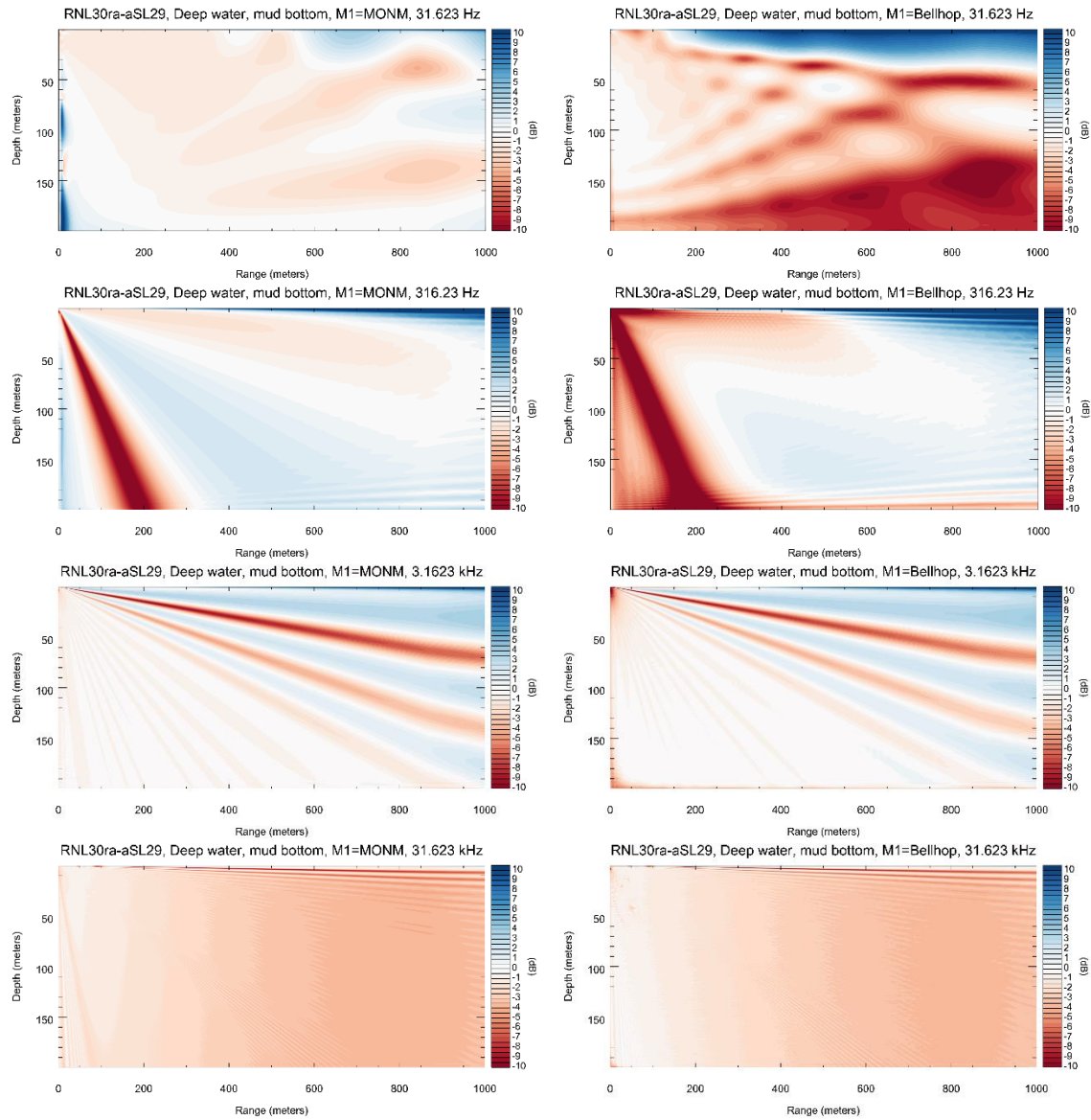


Figure 18. ddec RNL (Equation 37) – aSLo (Equation 31) versus range (m) and depth (m) for deep water (mud), in decibels. Left: MONM; right: BELLHOP.

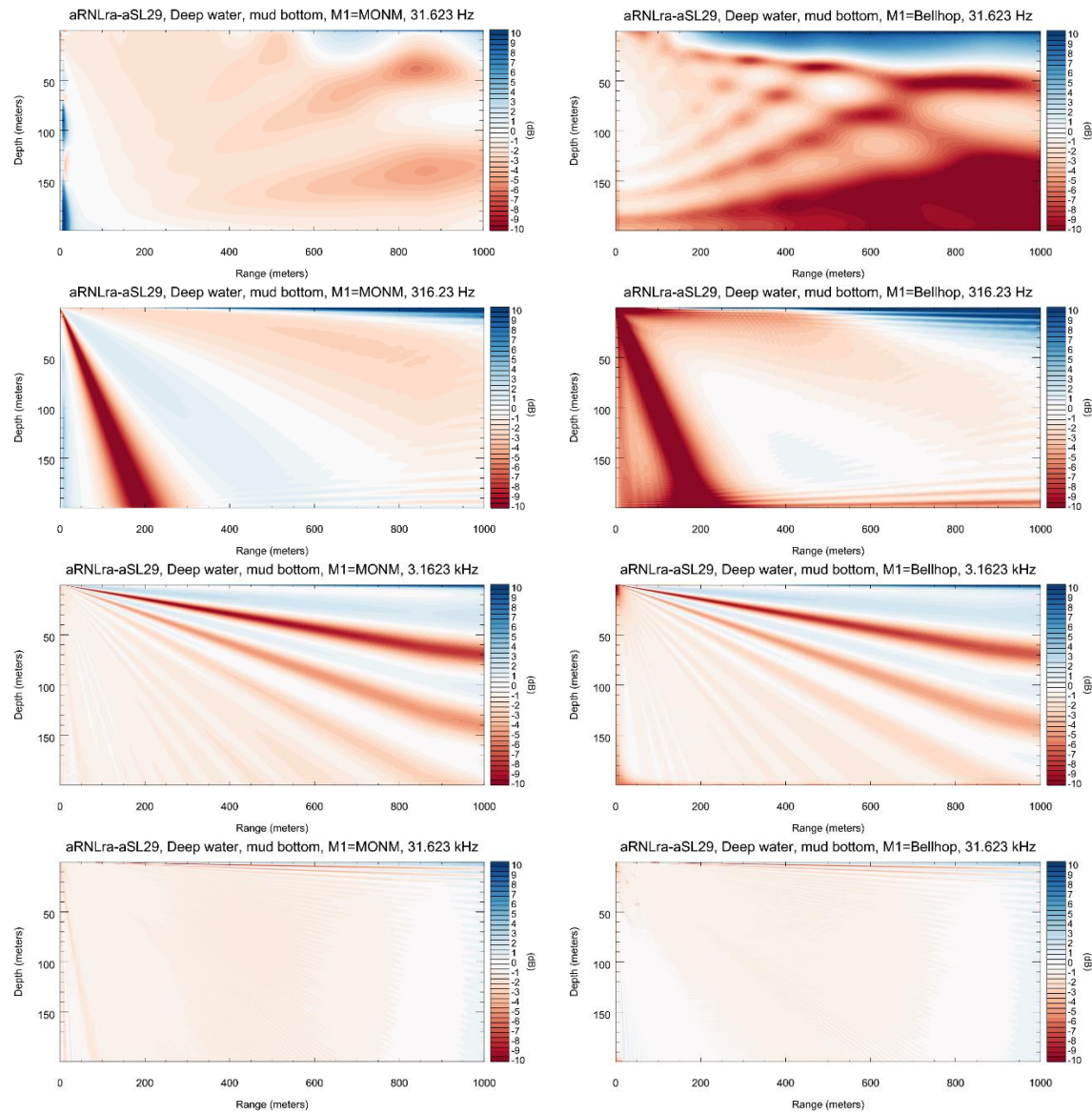


Figure 19. ddec aRNLa-aSL29 – aSL0 (Equation 31) versus range (m) and depth (m) for deep water (mud), in decibels. Left: MONM; right: BELLHOP.

### 2.7.1.4. SL

The deep fringe in RNL anomaly (Figure 18) at 300 Hz is caused by a robust null in the PL at this frequency (Figure 15) and is also present in the SL, though reversed in sign because the null in single frequency PL is deeper than for broadband (ddec) PL (Figure 20). The use of “MONM-MONM” in the caption (left-hand panels) indicates that MONM was used both for forward modelling, to estimate the ddec SPL field, and again for the inverse calculation, to estimate SL. For the right-hand panels, BELLHOP was used for both, as indicated by “BELLHOP-BELLHOP”.

The fringes at 3 kHz are barely visible in Figure 18, and their prominence in Figure 20 is attributed to the propagation loss term in Equation 42. In principle, these fringes can be removed by averaging over hydrophones, but an alternative is to average over frequency instead.

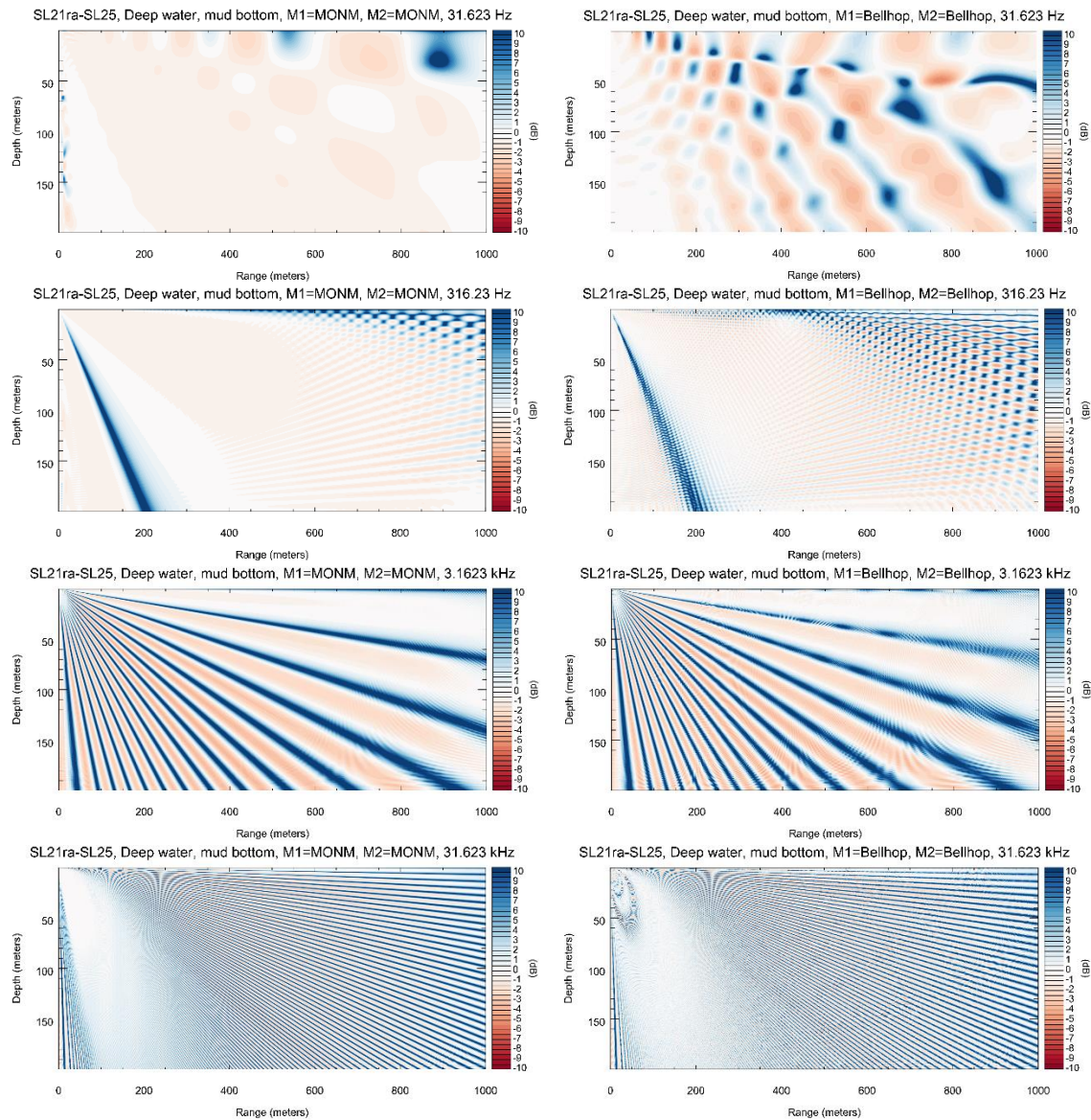


Figure 20. ddec SL (Equation 42) – SLo Equation (Equation 26) versus range (m) and depth (m) for deep water (mud), in decibels. Left: MONM-MONM; right: BELLHOP-BELLHOP.



The effect of averaging over frequency can be simulated by using an incoherent sum over rays for the PL term in Equation 42 instead of a coherent sum (Figure 21). The use of “MONM-BELLHOP” in the caption (left-hand panels) indicates that MONM was used for forward modelling, to estimate the ddec SPL field, while BELLHOP was used for the inverse calculation, to estimate SL. For the right-hand panels, an incoherent ray sum is carried out using the incoherent option in BELLHOP and indicated in figure captions (see Figures 21 and 30) by using “BELLINC” instead of “BELLHOP”. The effect is to weaken the 3 kHz fringes, but at the same time the 300 Hz feature reverses sign and deepens, suggesting that averaging in range or depth is needed at this frequency. Thus, BELLINC was used to estimate SL, still with MONM for the forward calculation, as indicated by “MONM-BELLINC”.

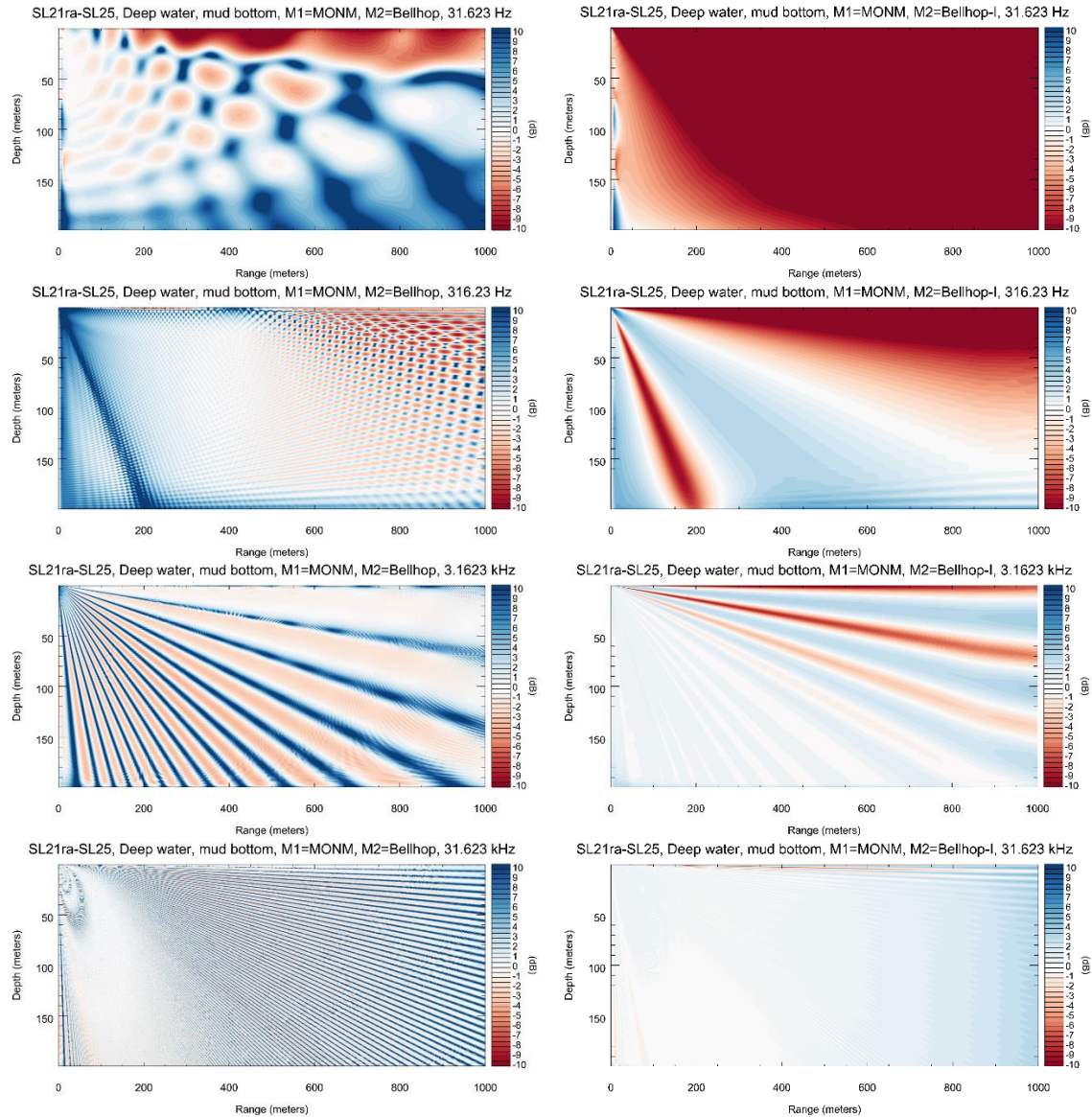


Figure 21. ddec SL (Equation 42) – SLo (Equation 26) versus range (m) and depth (m) for deep water (mud), in decibels. Left: MONM-BELLHOP; right: MONM-BELLINC

An alternative approach to soften the influence of interference fringes is to average in depth instead of in frequency. The plots in Figure 22 are obtained by evaluating Equation 47 at multiple heights above seafloor. For each height  $h$ , the field is averaged between depths  $H - h$  and  $H$ . When  $h$  is small (close to seabed), there is little averaging and the result is oscillatory. When  $h$  approaches  $H$ , the average is over entire water column, and the plots are smooth, with remaining variations in range corresponding (at long range) to cylindrical spreading. These graphs permit assessment of the relative benefit of averaging over (say) one quarter, one third, or one half of the water column.

In deep water, the cylindrical spreading starts at about 1 km (five water depths), so the benefits of depth averaging are not apparent from Figure 22. In shallow water (Section 2.7.2.4), the cylindrical spreading region starts at about 250 m, and there the effects are more visible (Figure 31).

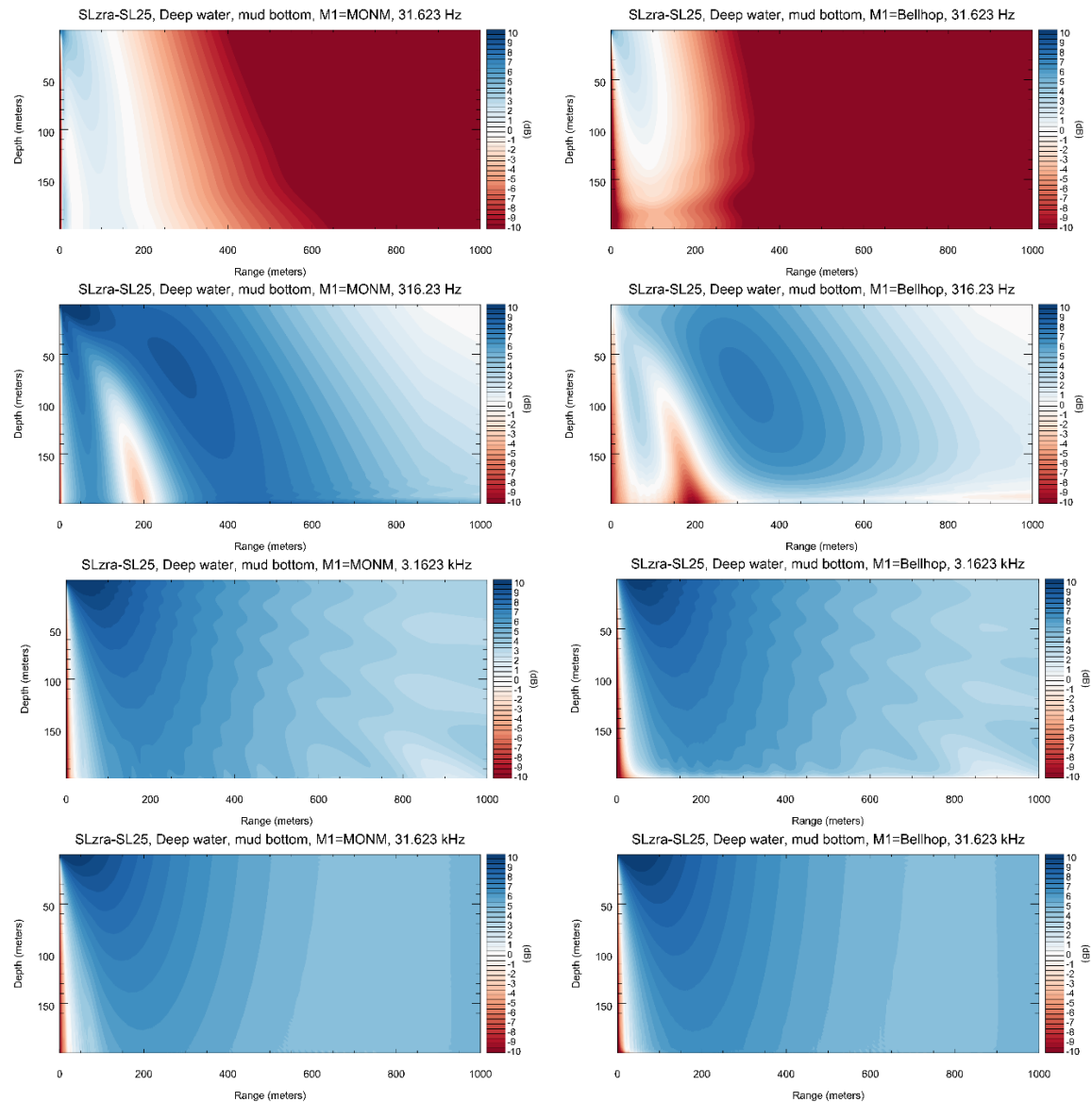


Figure 22. ddec HFSL (Equation 47) – SLo (Equation 26) versus range (m) and depth (m) for deep water (mud), in decibels. Left: MONM; right: BELLHOP.

## 2.7.2. Shallow Water: Mud and Sand

Shallow water results are presented using MONM, except where stated otherwise, for mud and sand sediments. The main reason for preferring MONM over BELLHOP is that the parabolic equation remains valid close to and even below the shallow water duct cut-off frequency (Jensen et al. 2011).

PL is calculated in cdec bands (Section 2.7.2.1, Figure 23). SPL is calculated in cdec and ddec bands (Section 2.7.2.2, Figures 25 and 26). The ddec band SPL includes a contribution from background noise (sea state 4, Figure 14) and is averaged in range in a way that simulates a vessel transit, for a 30° data window.

Multiple URN metrics are calculated from ddec band SPL in ddec bands (Sections 2.7.2.3 and 2.7.2.4). For each URN metric calculated using the methods described in Section 2.6, the calculated value (URN) is compared with the expected value (URN<sub>o</sub>) of that metric and plotted (Figures 27–31) in the form of the difference between the calculated and expected value ( $dURN = URN - URN_o$ ). These graphs show the difference  $dURN$  plotted versus horizontal range  $x$  and depth  $z$ . White indicates  $dURN = 0$ , while blue and red indicate  $dURN > 0$  and  $dURN < 0$ , respectively; the deeper the colour the larger the magnitude of  $dURN$ .

### 2.7.2.1. PL

Mud is a poor reflector of sound and consequently the PL for mud in shallow water Figure 23 left graph is similar to that for deep water zooming here (Figure 24 left) into the uppermost 50 m to facilitate comparison with Figure 23. For a sand seabed, more energy is reflected back into the water column, leading to lower PL for sand than for mud (Figure 23 right).

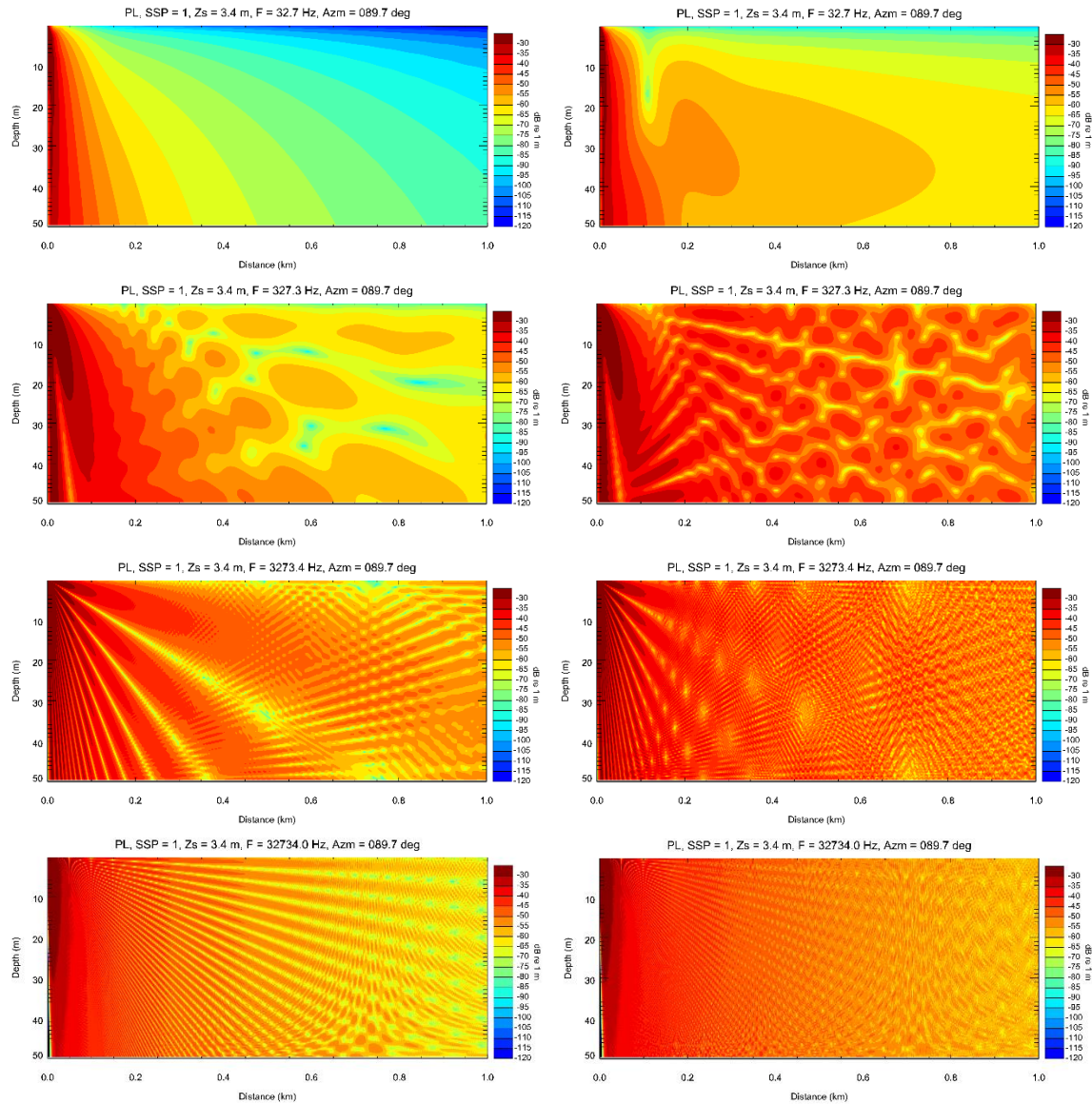


Figure 23. PL (Equation 21) re 1 m<sup>2</sup> versus range (m) and depth (m) for shallow water, in decibels. Left: mud; right: sand.

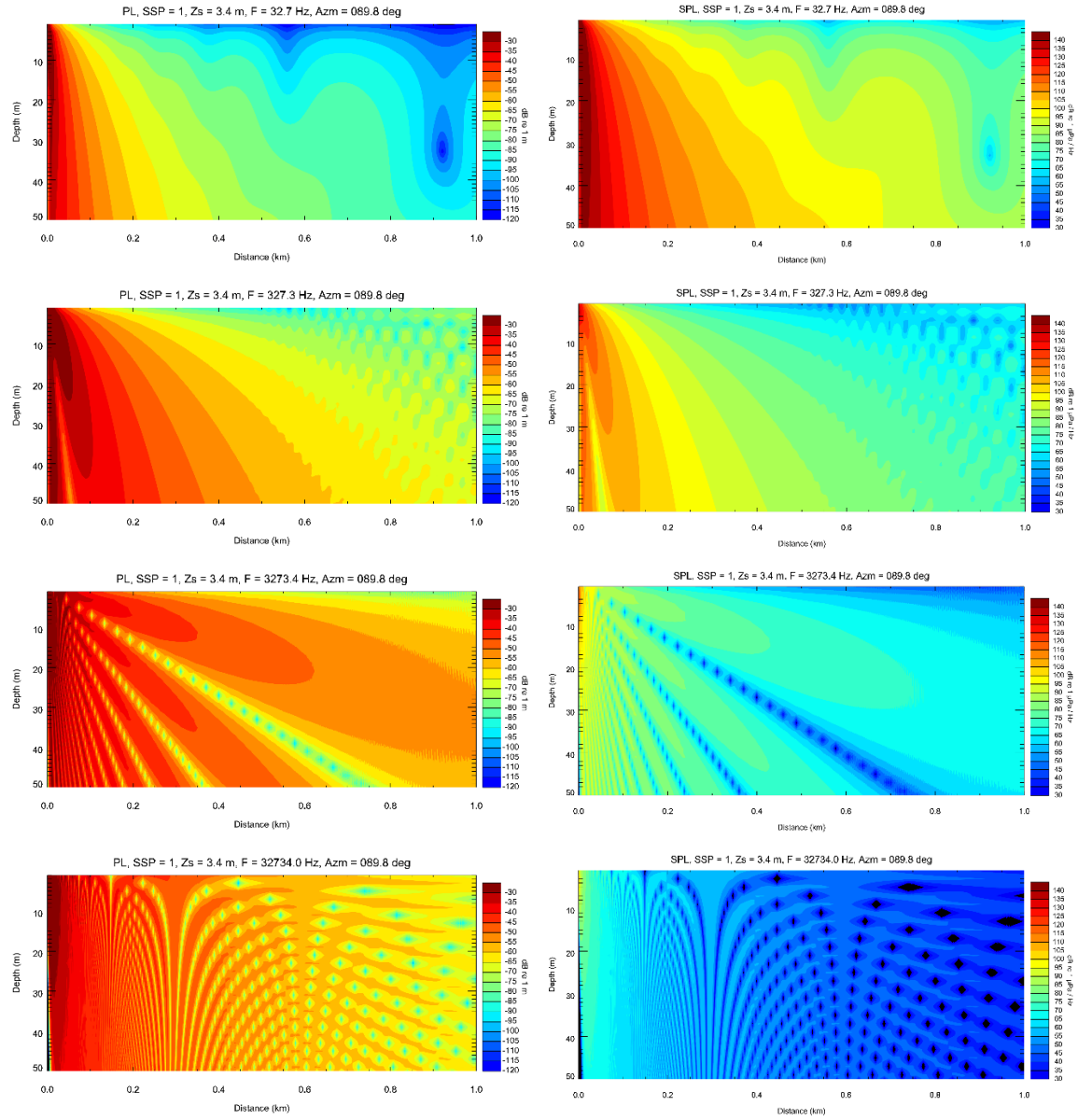


Figure 24. PL re 1 m<sup>2</sup> (dB) versus range (m) and depth (m) for deep water (mud). left: PL re 1 m<sup>2</sup> (dB). Right: cdec SPL (Equation 32) re 1 µPa<sup>2</sup> (dB).



### 2.7.2.2. SPL

The cdec SPL for mud (Figure 25 left) is similar to that for deep water (compare Figure 24 right). For sand, more energy reflected from seabed. Figure 26 shows the ddec SPL for mud (left) and sand (right). Again, as expected, propagation over sand in shallow water leads to higher SPL than propagation over mud (Figures 25 and 26).

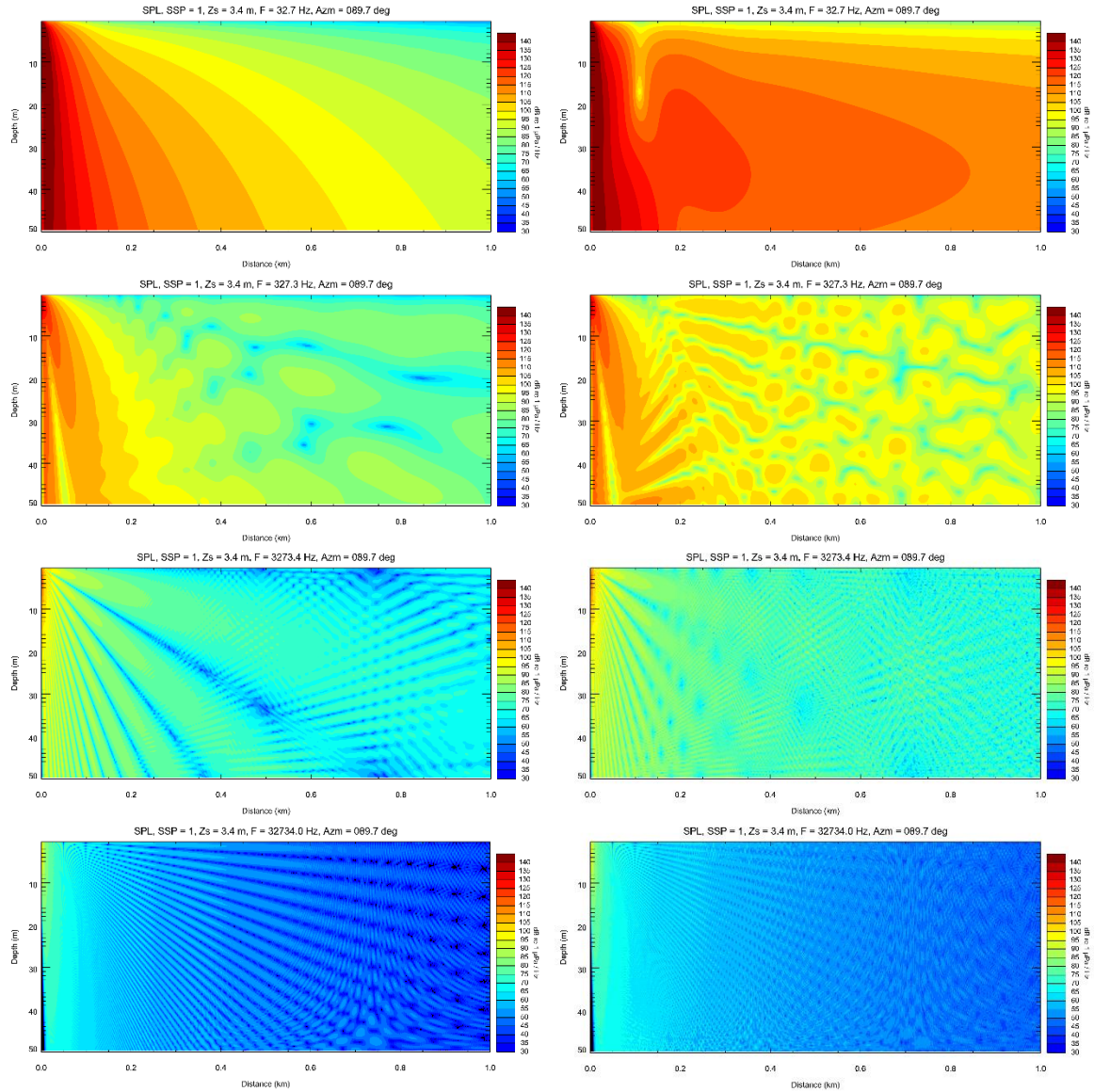


Figure 25. cdec SPL (Equation 32) re  $1 \mu\text{Pa}^2$  versus range (m) and depth (m) for shallow water, in decibels. Left: mud; right: sand.

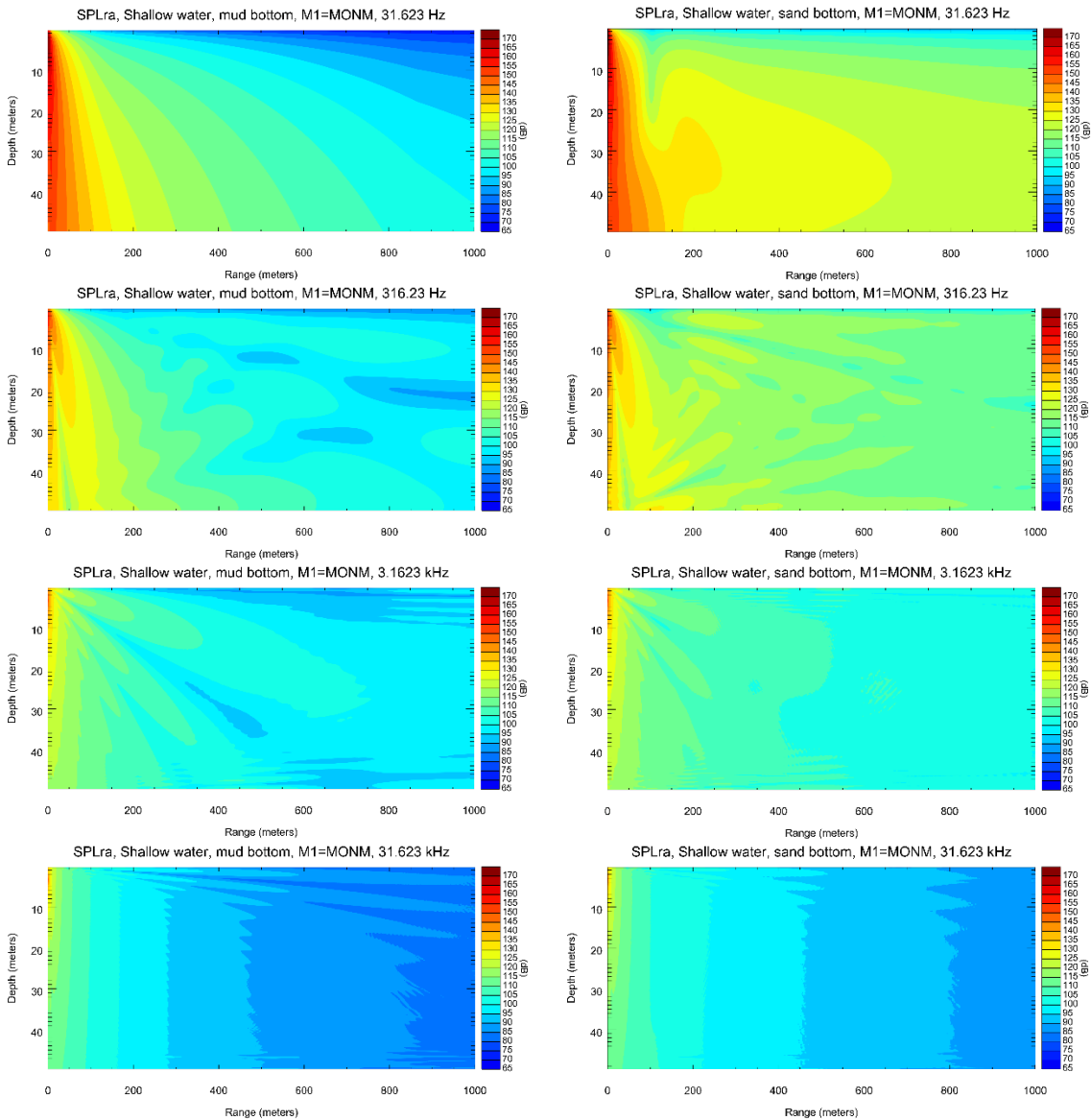


Figure 26. ddec SPL (Equation 34) re  $1 \mu\text{Pa}^2$  versus range (m) and depth (m) for shallow water, in decibels. Left: mud; right: sand. Decidecade (ddec) SPL includes contributions from both signal (sound from the vessel) and background noise, and is averaged over range to represent a  $\pm 30^\circ$  data window for a passing vessel.

### 2.7.2.3. RNL and aRNL

Figure 27 shows the RNL anomaly for mud (left) and sand (right). These graphs suggest that RNL can be inferred directly from ddec SPL measurements at the seabed up to 200 m range, at both low frequency (30 Hz) and high frequency (3 kHz and above), while further processing is required at intermediate frequencies, around 300 Hz.

Figure 28 shows the aRNL anomaly for mud (left) and sand (right). This quantity includes an adjustment for shallow water. The effect of the adjustment is to extend the region of applicability for aRNL to longer range than RNL.

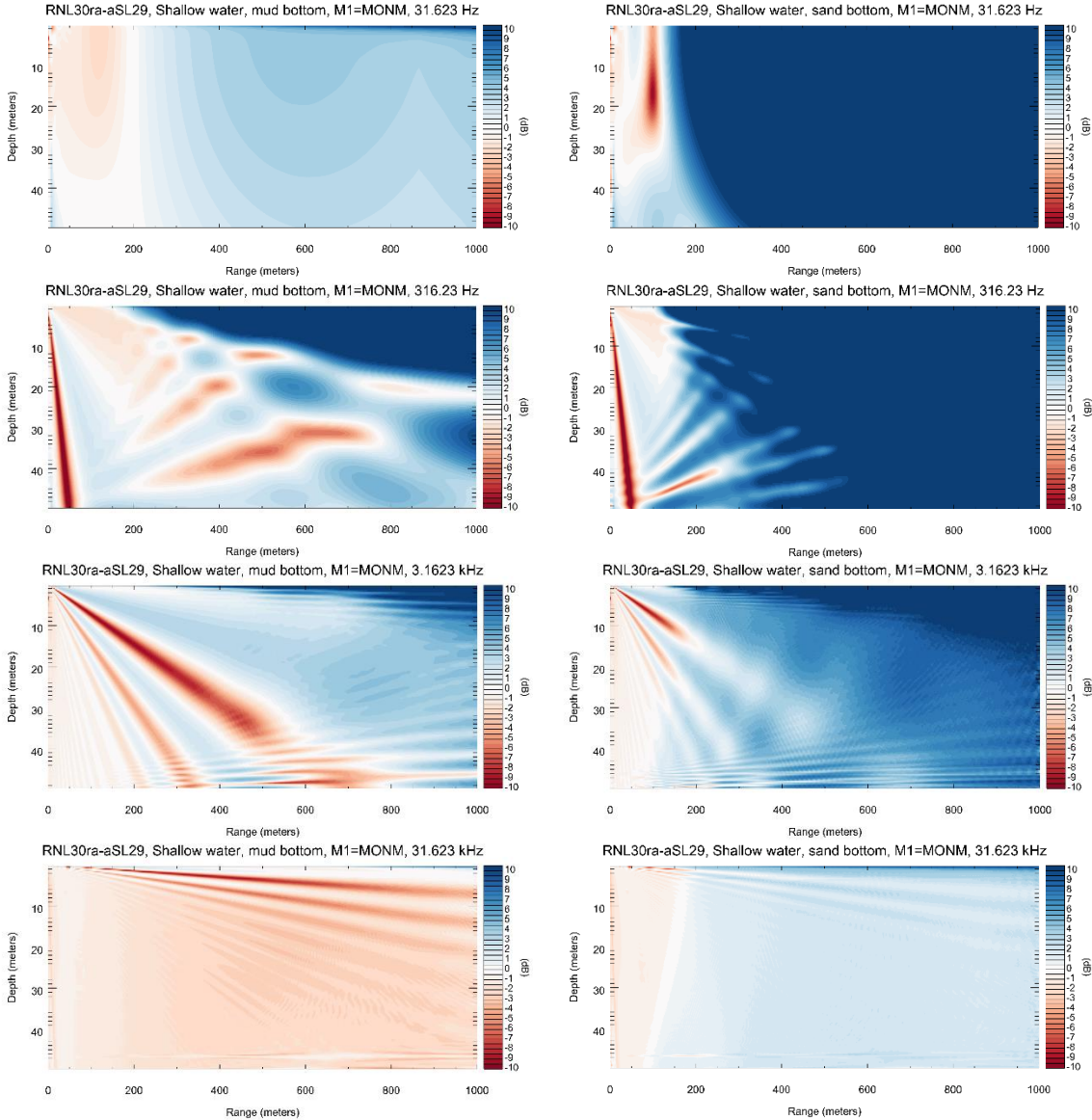


Figure 27. ddec RNL (Equation 37) – aSLo (Equation 31) versus range (m) and depth (m) for shallow water, in decibels. Left: mud; right: sand.



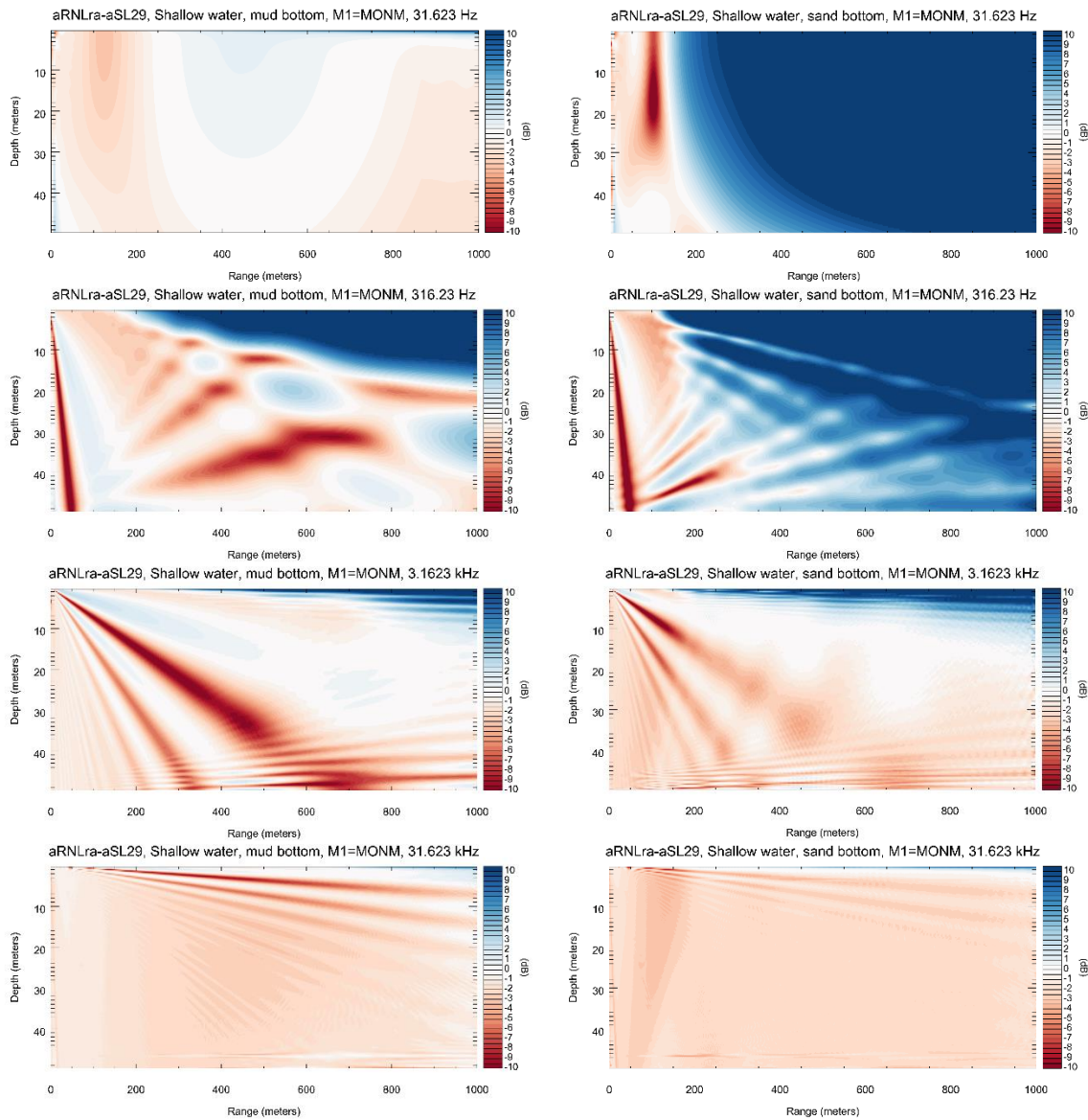


Figure 28. ddec aRNL (Equation 39) – aSLo (Equation 31) versus range (m) and depth (m) for shallow water, in decibels. Left: mud; right: sand.

### 2.7.2.4. SL

Figure 29 shows the SL anomaly for mud (left) and sand (right). The method works well at all frequencies, but it requires prior knowledge of seabed composition. Some averaging is also needed at most frequencies.

Figure 30 illustrates the effect of frequency averaging by means of an incoherent ray sum (BELLINC). This graph demonstrates the benefit of averaging over frequency.

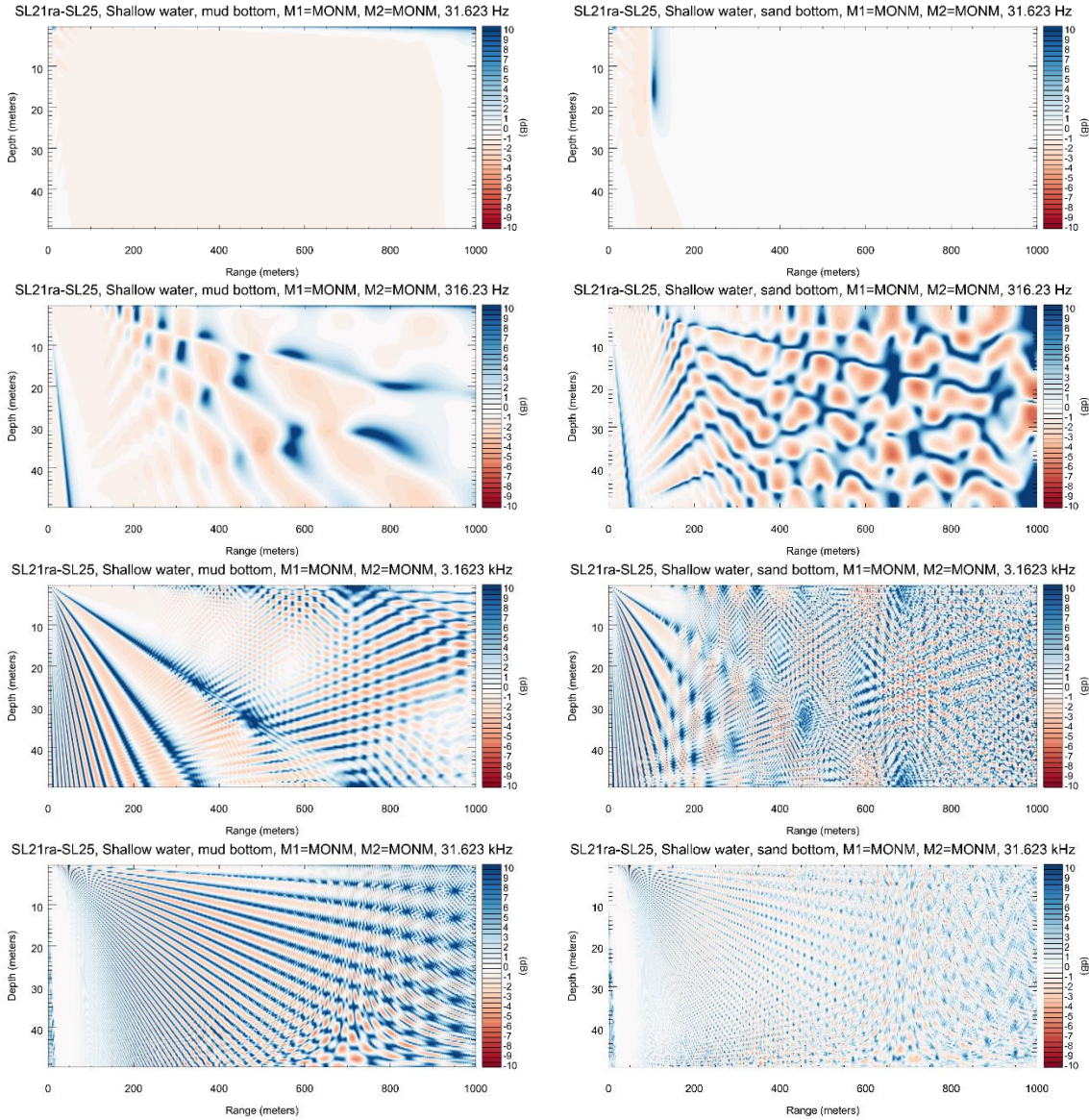


Figure 29. ddec SL (Equation 42) – SL<sub>0</sub> (Equation 26) versus range (m) and depth (m) for shallow water, in decibels. Left: mud; right: sand.

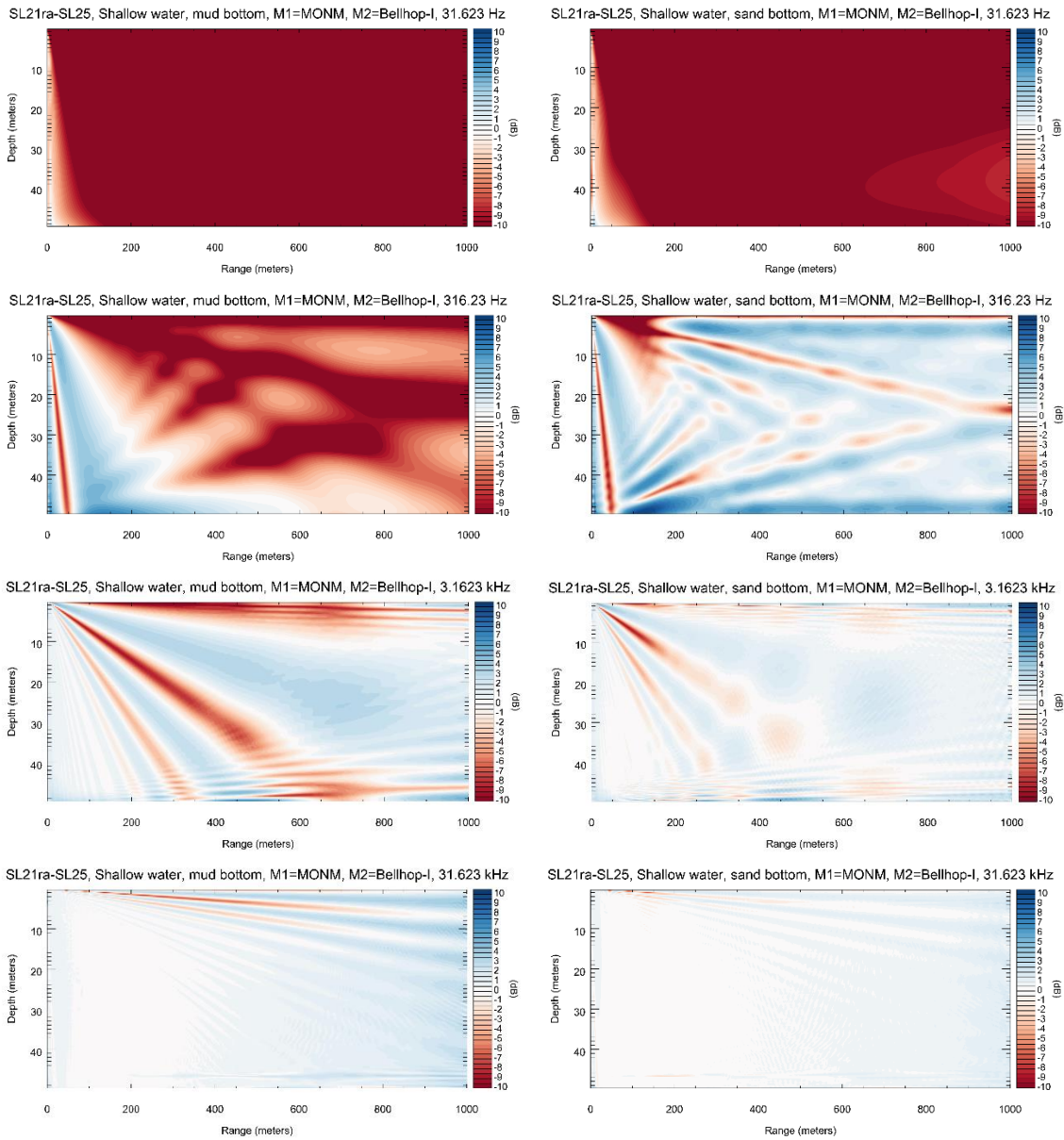


Figure 30. ddec SL (Equation 42) – SLo (Equation 26) versus range (m) and depth (m) using MONM-BELLINC, in decibels. Left: mud; right: sand

As with Figure 22, Figure 31 illustrates the effect of averaging in depth. The approach works well for sand at frequencies 300 Hz and above.

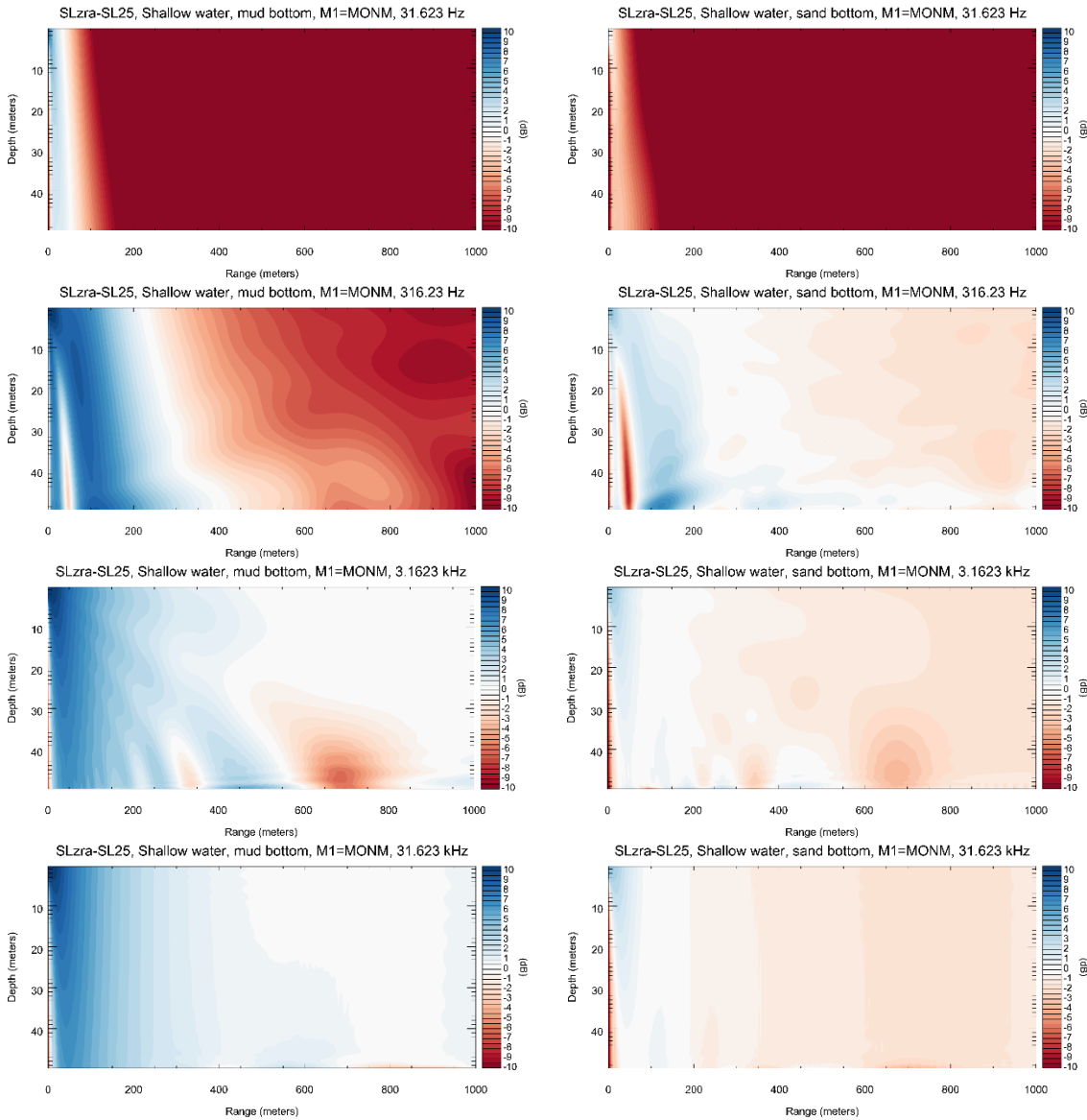


Figure 31. ddec HFSL (Equation 47) – SLO (Equation 26) versus range (m) and depth (m), in decibels. Left: mud; right: sand.



## Discussion and Conclusions

For each of the cases examined in the numerical experiments, observations are noted here about the effect of certain computational approaches on the estimation of various quantities. This provides insight into the optimal processing to be adopted when deriving vessel URN from field data collected in different experimental configurations and acoustic environments, thus enabling us to formulate some procedural recommendations for shallow water measurement approaches and geometries.

### 3.1. Deep Water (200 m, mud sediment)

#### 3.1.1. RNL and aRNL

The effect of averaging over frequency and range (Figures 17 and 18) is to smooth over interference features apparent in cdec SPL (Figure 16). This averaging is especially effective at 3 kHz, but at 300 Hz there remains a deep interference lobe caused by destructive interference between the direct and surface-reflected paths (Figure 18). The angle at which this happens is given by  $kd \sin \theta = \pi$ , from which we can calculate the range:

$$x = H\sqrt{4(df/c)^2 - 1}. \quad (49)$$

Substituting  $H = 200$  m,  $d = 3.4$  m,  $f = 316.2$  Hz and  $c = 1500$  m/s in Equation 46 gives  $x = 205$  m.

In reality, the interference nulls will be less deep, and therefore less problematic, than suggested by Figure 18 because a ship is not a point source.

The aRNL (Figure 19) is almost identical to RNL in deep water (Figure 18), as expected.

#### 3.1.2. SL

Interference features appear in SL (Figure 20) that are absent in RNL (Figure 18). The PL term in the equation  $SL = SPL + PL$  is evaluated at a single frequency, with no averaging. This introduces artefacts in the form of peaks in the estimated SL due to nulls in the single frequency interference pattern (Figures 18 and 19). The problem could be addressed by evaluating PL in 10 cdec bands and averaging over frequency, but we seek a simpler solution. One way to simulate the effect of averaging over frequency is to use an incoherent ray trace. Use of BELLINC to calculate PL removes the artificial peaks in SL at 3 kHz and above (Figure 21). At lower frequencies, a different approach would be needed.

An alternative approach to obtaining the high-frequency source level (HFSL) is to average the sound field over depth and apply cylindrical spreading. This approach overestimates SL in deep water (Figure 22) because in deep water we still have conditions approaching spherical spreading to a range of 1000 m.

## 3.2. Shallow Water (50 m, Mud and Sand Sediments)

### 3.2.1. RNL and aRNL

Receivers placed at a horizontal distance of between 100 and 200 m are well suited to measure RNL in shallow water, for both mud and sand sediments (Figure 27). The interference null observed at 300 Hz in deep water is also apparent in shallow water. Further processing is therefore needed at frequencies around 300 Hz. Possibilities include:

- *Average over frequency:* One approach is to average the field over more than one decade band. Averaging over (say) 3 or 5 ddec bands would help remove persistent interference features such as the propagation null at 300 Hz at angle  $\text{asin}(\pi/kd)$  (see e.g., Figures 26 and 27). This approach, which we recommend if measurements are limited to a single hydrophone, reduces band to band variability by smoothing over successive ddec bands.
- *Coherent processing:* The fringe can be removed by modelling the interference pattern in more detail than is done here. One approach is to use cdec band processing throughout instead of ddec bands. This also works for a single hydrophone, but is less robust than an incoherent average over frequency, requiring precise knowledge of the geometry and (possibly) of the seabed composition.
- *Average over multiple hydrophones:* If multiple hydrophones are available, these can be placed to sample the interference pattern to include both nulls and troughs. Effects of fringes are removed when one averages over the hydrophones. The averaging can be in range or depth or both.

The calculation of aRNL is effective at reproducing the deep water RNL value at frequencies 300 Hz and above. At 30 Hz, a different approach is needed.

### 3.2.2. SL

As in deep water, interference features appear in SL (Figure 29) that are absent in RNL (Figure 27), and for the same reason. Use of BELLINC to calculate PL removes the artificial peaks in SL at 3 kHz and above (Figure 30), implying that the fringes can be removed by averaging incoherently over frequency. At lower frequencies a coherent approach would be needed, involving an estimation of the Lloyd's mirror pattern at short range, or a coherent wave solution (parabolic equation, wave-number integration or normal mode) at long range.

An alternative approach, for obtaining the HFSL, is to average the sound field over depth and apply cylindrical spreading. This approach works well in shallow water at ranges between 200 and 400 m (Figure 31) at 300 Hz and above, especially for sand. The approach also works for mud at 3 kHz and above. Bearing in mind the inevitable decrease in SNR at longer ranges, this suggests an optimal range of about five water depths.

## 3.3. Preferred Processing

The most appropriate processing depends on hydrophone geometry and application. Measurement of RNL seems feasible at close range, especially for a mud sediment, although one hydrophone seems unlikely to be sufficient. An alternative for consideration at longer ranges and high frequency is aRNL. At low frequency (and long range), the best approach for quiet ship certification is probably to calculate aSL.

The authors have the impression that the focus of ISO 17208-3 is on SL. The remainder of this section concentrates on measurement of SL and the preferred processing method as a function of hydrophone geometry.

### 3.3.1. Single Hydrophone

A good place for single hydrophone measurements is at the seabed, as close as possible to the vessel track consistent with staying in the source's acoustic far field. Some frequency averaging (e.g., by means an incoherent ray sum) is likely needed at 3 kHz and above to remove interference. At 300 Hz and below, a coherent method is needed, involving estimation of the Lloyd's mirror interference pattern.

### 3.3.2. Vertical Array at Five Water Depths from the Vessel

At 3 kHz and above, one can use a depth average. At 300 Hz and below, a coherent method is needed, involving an estimation of the coherent wave solution (parabolic equation, wave-number integration, or normal mode) at long range.

### 3.3.3. Horizontal Array on Seabed

At 3 kHz and above, one can use a range average. At 300 Hz and below, a coherent method is likely needed, involving estimation of the Lloyd's mirror interference pattern.

## 3.4. Implications of a Harder Sediment in Shallow Water

The shallower the water, the higher the likelihood of there being a hard sediment or bedrock basement beneath a fine sediment layer of mud or fine sand. The existence of such a hard basement would increase the low-frequency reflectivity and critical angle of the seabed relative to those for a fine sediment. Stronger reflections at short range would contaminate the measurement of RNL at short range and tilt the balance in favour of aRNL, which would correct for these reflections. Use of SL (or aSL) would be unaffected if the seabed is well characterized. The cylindrical spreading method used to estimate HFSL should become more robust with a large critical angle.

The authors see no reason a priori reason to expect a different conclusion regarding the optimum geometry. However, knowledge of the sediment type (especially of the critical angle, which can be measured during the planned PL experiment), is vital to a successful characterization of vessel URN in shallow water. The simplest approach to obtain the critical angle is to measure mean-square sound pressure ( $P$ ) vs range ( $r$ ) from a broadband source using a single hydrophone. At short range (and high frequency) these are related according to spherical spreading,  $P = 2/r^2$ . At long range this becomes cylindrical spreading,  $2\psi/(rH)$ , where  $H$  is the water depth. Using  $R$  to denote the range at which the two lines cross, the critical angle is  $\psi = H/R$ . If the source is calibrated the short range data are not needed, and one can calculate  $\psi$  instead as  $PrH/(2S)$ , where  $S$  is the (known) source factor. During the PL experiment we will evaluate  $\psi$  both ways as a cross-check. At low frequency one needs to account for the dipole nature of the source as described earlier in this White paper (see also Ainslie et al. 2014).  
Recommendations for URN Measurement Procedures

In shallow water (say 30 m water depth), three or more hydrophones should be placed at the seabed, with CPA approximately equal to one ship length. The closest hydrophone is at a null of some frequency determined by  $kd \sin \theta = \pi$ . Place a second hydrophone at the peak ( $kd \sin \theta = \pi/2$ ). If you have a third hydrophone, place it between these ( $kd \sin \theta = 3\pi/4$ ). The purpose is to place the receivers in the direct path, and thus reduce sensitivity to (likely unknown) seabed composition by minimising the relative contribution from bottom-reflected paths.

In intermediate water depth (say 70 m), three or more equally spaced hydrophones should be placed in a vertical array, spanning at least half of the water column, at a CPA of about five water depths. The purpose is to place the receivers in the cylindrical spreading region, and thus reduce sensitivity to detailed interference patterns by averaging over depth.

Propagation loss measurements using a controlled sound source should be conducted during the field experiment to measure the seabed properties.

## Literature Cited

- [IEC] International Electrotechnical Commission. 2014. *IEC 61260-1:2014 Electroacoustics - Octave-band and fractional-octave-band filters - Part 1: Specifications*. <https://www.iso.org/standard/62406.html>.
- [ISO] International Organization for Standardization. 2016. *ISO 17208-1:2016. Underwater acoustics – Quantities and procedures for description and measurement of underwater sound from ships – Part 1: Requirements for precision measurements in deep water used for comparison purposes*. <https://www.iso.org/standard/62408.html>.
- [ISO] International Organization for Standardization. 2017. *ISO 18405:2017. Underwater acoustics – Terminology*. Geneva. <https://www.iso.org/standard/62406.html>.
- [ISO] International Organization for Standardization. 2019. *ISO 17208-2:2019 Underwater acoustics — Quantities and procedures for description and measurement of underwater sound from ships — Part 2: Determination of source levels from deep water measurements*.
- Ainslie, M.A. 2010. *Principles of Sonar Performance Modeling*. Praxis Books. Springer, Berlin. <https://doi.org/10.1007/978-3-540-87662-5>.
- Ainslie, M.A., P.H. Dahl, C.A.F. de Jong, and R.M. Laws. 2014. *Practical Spreading Laws: The Snakes and Ladders of Shallow Water Acoustics. UA2014 - 2nd International Conference and Exhibition on Underwater Acoustics*, 22-27 Jun 2014, Island of Rhodes, Greece, pp. 879-886.
- Ainslie, M.A., J.L. Miksis-Olds, S.B. Martin, K.D. Heaney, C.A.F. de Jong, A.M. von Benda-Beckmann, and A.P. Lyons. 2018. *ADEON Underwater Soundscape and Modeling Metadata Standard*. Version 1.0. Technical report by JASCO Applied Sciences for ADEON Prime Contract No. M16PC00003. <https://doi.org/10.6084/m9.figshare.6792359.v2>.
- Ainslie, M.A., D.E. Hannay, A.O. MacGillivray, and K. Lucke. 2020. *Proposed Alignment of Measurement and Analysis for Quiet Ship Certifications*. Document Number 02024, Version 4.0. Technical memorandum by JASCO Applied Sciences for Vancouver Fraser Port Authority.
- ANSI S1.11-2004. R2009. *American National Standard Specification for Octave-band and Fractional-octave-band Analog and Digital Filters*. Acoustical Society of America.
- ANSI S1.1-1994. R2004. *American National Standard Acoustical Terminology*. American National Standards Institute, NY, USA.
- ANSI/ASA S12.64/Part 1. 2009. *American National Standard Quantities and Procedures for Description and Measurement of Underwater Sound from Ships Part 1: General Requirements*. American National Standards Institute and Acoustical Society of America, NY, USA.
- Collins, M.D. 1993. A split-step Padé solution for the parabolic equation method. *Journal of the Acoustical Society of America* 93(4): 1736-1742. <https://doi.org/10.1121/1.406739>.
- Collins, M.D., R.J. Cederberg, D.B. King, and S. Chin-Bing. 1996. Comparison of algorithms for solving parabolic wave equations. *Journal of the Acoustical Society of America* 100(1): 178-182. <https://doi.org/10.1121/1.415921>.
- de Jong, C.A.F., M.A. Ainslie, J. Dreschler, E. Jansen, E. Heemskerk, and W. Groen. 2010. *Underwater noise of Trailing Suction Hopper Dredgers at Maasvlakte 2: Analysis of source levels and background noise*. Document Number TNO-DV 2010 C335. TNO.
- Fisher, F.H. and V.P. Simmons. 1977. Sound absorption in sea water. *Journal of the Acoustical Society of America* 62(3): 558-564. <https://doi.org/10.1121/1.381574>.



- François, R.E. and G.R. Garrison. 1982. Sound absorption based on ocean measurements: Part II: Boric acid contribution and equation for total absorption. *Journal of the Acoustical Society of America* 72(6): 1879-1890. <https://doi.org/10.1121/1.388673>.
- Hannay, D.E., A.O. MacGillivray, H. Frouin-Mouy, Z. Li, F. Pace, J.L. Wladichuk, and Z. Alavizadeh. 2019. *Study of Quiet-Ship Certifications: Analysis using the ECHO Ship Noise Database*. Document Number 01737, Version 1.0. Technical report by JASCO Applied Sciences for Transport Canada.
- Jensen, F.B., W.A. Kuperman, M.B. Porter, and H. Schmidt. 2011. *Computational Ocean Acoustics*. 2nd edition. AIP Series in Modern Acoustics and Signal Processing. AIP Press - Springer, New York. 794 p. <https://doi.org/10.1007/978-1-4419-8678-8>.
- Miksis-Olds, J.L., D.L. Bradley, and X.M. Niu. 2013. Decadal trends in Indian Ocean ambient sound. *Journal of the Acoustical Society of America* 134(5): 3464-3475. <https://doi.org/10.1121/1.4821537>.
- Porter, M.B. and Y.C. Liu. 1994. Finite-element ray tracing. In: Lee, D. and M.H. Schultz (eds.). *International Conference on Theoretical and Computational Acoustics*. Volume 2. World Scientific Publishing Co. pp. 947-956.
- Robinson, S.P., P.D. Theobald, G. Hayman, L.-S. Wang, P.A. Lepper, V.F. Humphrey, and S. Mumford. 2011. *Measurement of Underwater Noise Arising from Marine Aggregate Dredging Operations: Final Report*. Document Number 09/P108. Marine Environment Protection Fund (MEPF). <https://webarchive.nationalarchives.gov.uk/20140305134555/http://cefas.defra.gov.uk/alsf/projects/direct-and-indirect-effects/09p108.aspx>.
- Wales, S.C. and R.M. Heitmeyer. 2002. An ensemble source spectra model for merchant ship-radiated noise. *Journal of the Acoustical Society of America* 111(3): 1211-1231. <https://doi.org/10.1121/1.1427355>.
- Wenz, G.M. 1962. Acoustic Ambient Noise in the Ocean: Spectra and Sources. *Journal of the Acoustical Society of America* 34(12): 1936-1956. <https://doi.org/10.1121/1.1909155>.
- Zhang, Z.Y. and C.T. Tindle. 1995. Improved equivalent fluid approximations for a low shear speed ocean bottom. *Journal of the Acoustical Society of America* 98(6): 3391-3396. <https://doi.org/10.1121/1.413789>.

## Appendix A. Standard Frequency Bands

Standard bands are arranged logarithmically in frequency and are based on powers of ten around a centre frequency of 1000 Hz. Multiplying this centre frequency by integer powers of ten gives 10, 100, 1000, and 10,000 Hz. The band between each successive factor of 10 (e.g., from 100 to 1000 kHz) is a decade. It is customary to divide each decade band into ten equal sub-bands, each one tenth of a decade (i.e., one decidecade) wide. Table A-1, based on the *ADEON Soundscape Specification* (Ainslie et al. 2018), shows decidecade (ddec) bands according to IEC (2014), for decidecade frequency bands with centre frequencies 10 Hz ( $n = -20$ ) Hz to 100 kHz ( $n = +20$ ). Each decidecade band in the table is identified by a unique integer index between  $n = -20$  (10 Hz) and  $+20$  (100 kHz), with  $n = 0$  corresponding to 1 kHz.

Table A-1. Decidecade frequency bands, as defined by IEC (2014), with centre frequencies between 10 Hz ( $n = -20$ ) and 100 kHz ( $n = +20$ ). Band edge and centre frequencies are stated to five significant figures. Centre frequencies of nominal octave bands (the precise bandwidth of which is 3 ddec) are bold. Alternate light and dark shading shows ADEON decade bands B to E (Ainslie et al. 2018).

Band index ( $n$ )	Lower bound ( $f_{\min}/\text{Hz}$ )	Centre frequency ( $f_c/\text{Hz}$ )	Upper bound ( $f_{\max}/\text{Hz}$ )	Nominal centre frequency ( $f_{c,\text{nom}}/\text{Hz}$ )
-20	8.9125	10.000	11.220	10
-19	11.220	12.589	14.125	12.5
-18	14.125	<b>15.849</b>	17.783	16
-17	17.783	19.953	22.387	20
-16	22.387	25.119	28.184	25
-15	28.184	<b>31.623</b>	35.481	32
-14	35.481	39.811	44.668	40
-13	44.668	50.119	56.234	50
-12	56.234	<b>63.096</b>	70.795	63
-11	70.795	79.433	89.125	80
-10	89.125	100.00	112.20	100
-9	112.20	<b>125.89</b>	141.25	125
-8	141.25	158.49	177.83	160
-7	177.83	199.53	223.87	200
-6	223.87	<b>251.19</b>	281.84	250
-5	281.84	316.23	354.81	320
-4	354.81	398.11	446.68	400
-3	446.68	<b>501.19</b>	562.34	500
-2	562.34	630.96	707.95	630
-1	707.95	794.33	891.25	800
0	891.25	<b>1000.0</b>	1122.0	$1 \cdot 10^3$
1	1122.0	1258.9	1412.5	$1.25 \cdot 10^3$
2	1412.5	1584.9	1778.3	$1.6 \cdot 10^3$
3	1778.3	<b>1995.3</b>	2238.7	$2 \cdot 10^3$
4	2238.7	2511.9	2818.4	$2.5 \cdot 10^3$

Band index (n)	Lower bound ( $f_{\min}$ /Hz)	Centre frequency ( $f_c$ /Hz)	Upper bound ( $f_{\max}$ /Hz)	Nominal centre frequency ( $f_{c,nom}$ /Hz)
5	2818.4	3162.3	3548.1	$3.2 \cdot 10^3$
6	3548.1	<b>3981.1</b>	4466.8	$4 \cdot 10^3$
7	4466.8	5011.9	5623.4	$5 \cdot 10^3$
8	5623.4	6309.6	7079.5	$6.3 \cdot 10^3$
9	7079.5	<b>7943.3</b>	8912.5	$8 \cdot 10^3$
10	8912.5	10000	11220	$10 \cdot 10^3$
11	11220	12589	14125	$12.5 \cdot 10^3$
12	14125	<b>15845</b>	17783	$16 \cdot 10^3$
13	17783	19953	22387	$20 \cdot 10^3$
14	22387	25119	28184	$25 \cdot 10^3$
15	28184	<b>31623</b>	35481	$32 \cdot 10^3$
16	35481	39811	44668	$40 \cdot 10^3$
17	44668	50119	56234	$50 \cdot 10^3$
18	56234	<b>63096</b>	70795	$63 \cdot 10^3$
19	70795	79433	89125	$80 \cdot 10^3$
20	89125	100000	112200	$100 \cdot 10^3$

A decade (0.1 dec) is approximately equal to one third of an octave, and for this reason is referred to by IEC (2014) as a “one-third octave” (Table A-2).

Table A-2. Fractional octave and fractional decade frequency bands.

Frequency ratio	IEC 61260:1995	IEC 61260-1:2014	ISO 18405	ISO 80000-8	Notes
2	octave	-	octave	octave	
$2^{1/3}$	one-third octave	-	one-third octave one-third octave (base 2)		
10	-	-	decade	decade	
$10^{1/10}$	one-third octave	one-third octave	decidecade one-third octave (base 10)		an alternative name for this frequency ratio is “one-tenth decade” (ANSI S1.6-2016)

## Appendix B. WG1 Bibliography

This bibliography was provided by the Convenor of WG1, Christian Audoly on 12 August 2020.

### **ISO TC 43/SC 3 – WG1 - Ship radiated measurement**

#### **Underwater acoustics — Quantities and procedures for description and measurement of underwater noise from ships Part 3: Requirements for measurements in shallow waters**

#### **Bibliography**

#### **Version 2 – 12 August 2020**

This document lists bibliographic references that can be useful for deriving a standard for ship radiated noise measurement in shallow waters, and provides a summary of the contents. The items are listed in chronological order, distinguishing:

- Work done by members of the WG, and
- Other documents.

### **B.1. Work Done by Members of the WG**

- [1] **Lian Wang, Stephen Robinson, and Pete Theobald, Calculation of ship source level in shallow water by propagation modelling. Internoise 2016, Hamburg**

In this paper, a comparison of propagation modelling results (using different models) for a measurement setup in shallow waters is described, and some sources of uncertainty are identified. Monte Carlo simulations were carried out to examine the effects of variable environmental conditions with a given measurement configuration.

- [2] **Lian Wang and Stephen Robinson, A comparison of methods for measuring ship source level in shallow water. ICSV24, London, 23–27 July 2017**

This paper introduces the topic and there is a discussion of the main driving parameters. The main source of uncertainty is in the propagation loss term. A figure suggests a measurement configuration with one hydrophone and combination of measurements at different distances.

- [3] **“ShallowWaterPropagationSimulationsModelComparison20180514” (Excel file), May 2018**

Excel file giving a cross-comparison of simulation results, for a given water depth (60 m) and different distances, from three different teams:

- NPL (L. Wang, S. Robinson): Model OASES;
- TNO (C. de Jong): Image method; and
- Naval Group (V. Meyer, C. Audoly): Scooter&Fields < 1000 Hz, Bounce&Bellhop >=1000 Hz.

In general, there is little difference between the models, except at very low frequency in some cases.

**[4] V. Meyer, Simulation of ship radiated noise measurement in shallow waters – Parametric study for the influence of environment and sensor configuration. Technical report Naval Group CRT/CEMIS/R-18013 Issue A, June 2018**

The objective is to realize a parametric study framework to evaluate by simulation the influence of some environmental parameters and sensor configurations on the propagation correction terms in the ship radiated noise measurement in shallow waters. The source is assumed to be an omnidirectional point source located at depth  $z_s$  below the sea surface, and the measurement is done using a vertical array at some distance from the ship.

The main conclusions are:

- At low frequency, dominant effect of Lloyd's mirror effect, similar to the deep waters case;
- Little influence of sound speed profile in the water column, if measurement distance is not too large;
- Influence of water depth, measurement distance and seafloor properties; and
- In the case of a sandy uniform seafloor, an analytical model is proposed for the propagation correction term, matching rather well numerical simulations.

**[5] Yin Cen, Monitoring Stations for Underwater Noise from Shipping. MSc Thesis, University of Southampton, August 2018**

In this project, a simulation program based on the image source model was developed to analyze the problem. It is assumed that the sea surface is rough and the seabed is level and smooth with a reflection coefficient that is a function of the incident angle and the attenuation in the sediment. The calculations are performed over a frequency range from 10 Hz to 1000 kHz with the results being averaged over one-third octave bands.

The conclusions are:

- Number of hydrophones: When the number of hydrophones changes from 3 to 5, the correction factor curve becomes significantly smoother. But when it changes from 5 to 15, the change of the correction factor curve is not so large.
- Location of hydrophones: The distribution of the correction factor is related to the angle between the sea surface and the line linking the ship and the hydrophone. Suggest that location of hydrophones could be specified by angles rather than depths.
- Number of image sources to be used in the model: 100 is quite sufficient.
- Influence of sea surface roughness: It has a significant impact on the correction factor. When the roughness increase, the correction factor decreases and the effect is greater at high frequency.

**[6] Yezhen Pang, Updates for full scale measurements. Technical presentation, 27–28 March 2019**

This presentation includes two topics, the surface reflection correction term in deep waters, and shallow waters measurements.

In a first part, a review of different existing procedures (ISO, BV, DNV, RINA, etc.) is done, with comparison on specified array geometry, ship sail track, and correction terms.

Some additional simulations are done in the shallow water case and compared to the previous results of the members of the WG. There is deviation at low frequency in one of the study cases.

The last part of the presentation shows results of a measurement campaign in real environment using a transducer for sound source, and a vertical array with numerous hydrophones at reception. The water depth is 55 to 40 m and distance up to 500 m. It is recommended to combine information from three different measurement distances. An averaged propagation factor can be used above 200 Hz. At lower frequency, a propagation numerical model must be used.

- [7] **V. Meyer and C. Audoly, Influence of the measurement configuration for the assessment of underwater noise radiated from ships in shallow water. IEEE-MTS Oceans 2019, Marseille, 17–20 June 2019**

Presents results from technical report [4] in a more synthetic form.

- [8] **Victor Humphrey, Yin Cen, Stephen Robinson, and Liansheng Wang, International standards for the measurement of underwater noise from vessels: numerical modelling in support of a shallow water standard. 178th ASA meeting, San Diego, 2019**

This talk has two aims: review the development of international standards for the measurement of radiated noise from ships, and to describe some of the undergoing work for the development of standard applicable to shallow water. The key point is the difference between the radiated noise level and the source level. Some measurement approaches only correct for geometrical spreading: it is the radiated noise level. It is useful for comparing vessels or monitoring changes. Others attempt to correct for presence of water surface, and seabed if applicable: it is the source level. This is useful if you want to obtain noise maps. The first standard in that sense was defined by ANSI in 2009, reused by the ISO technical committee for underwater acoustics to publish a standard in 2016 for the measurement of radiated noise in deep waters. In 2019, the part 2 was published to estimate source levels from deep water radiated noise measurement. Now the aim is to determine source levels from shallow water measurements. In parallel, classification societies have also developed procedures to determine noise source levels. Different possibilities are considered to compensate for shallow water effects: calibrate environment using active source, use propagation loss for each hydrophone using an appropriate propagation model or to define other corrections. Comparison with a simple formula proposed by Meyer and Audoly [4] shows good results for a sandy seafloor, but that there are deviations in other cases.

- [9] **Hans Hasenpflug, Anton Homm, Stefan Schäl, Layton Gilroy, Evaluation of range standards for underwater radiated noise in beam aspect. Proceedings of the 23rd International Congress on Acoustics in Aachen, Germany, 9–13 September 2019**

The underwater radiated noise levels of a small naval vessel were measured at the Heggernes deep water sound range. The data evaluation and analysis were performed in accordance with the NATO standard STANAG 1136 and the ISO 17208-1 standard. Both standards describe procedures for the determination of underwater radiated noise levels of ships in beam aspect on a deep water sound range. To assess and compare the results of both standards, the hydrophone configuration at the Heggernes range was utilized at various depth settings. Measurements were made of the ship in two different ship conditions (machinery states) and a variety of sailing speeds. Some of these measurements were repeated a large number of times. The resulting 3rd octave based spectra are used to compare the two procedures.

The DWL suggested by STANAG is too large for small ships and leads to 1 dB lower RNL compared to the DWL defined by ISO and used at Heggernes. Thus, for small ships, the DWL should be related to the ship length. RNL measured with a single hydrophone at shallow water depths, as specified by STANAG are lower, compared to the ISO 17208 standard due to the Lloyd's Mirror effect. RNL measured with a single hydrophone at 60 meters depths are comparable to the RNL of ISO. Both, the ISO and STANAG procedures should be reconsidered with respect to the definition of the DWL for small ships. A DWL related to the ship length, especially for small ships, is a more suitable approach. In order to achieve comparable RNL with ISO, measurements with a single hydrophone should be carried out at an aspect angle of 30° which corresponds to a measurement depth of circa 60 meters at a CPA distance of 100 m.

## B.2. Other Documents

**[10] Silent Class Notation, Det Norske Veritas (DNV), Rules for Ships, January 2010, Pt 6, Ch. 2, 2010**

Procedure recommended by the DNV for the determination of underwater ship radiated noise.

- Shallow waters, water depth greater than 30 m, sloping seafloor, flat floor admitted;
- Single hydrophone near seafloor;
- Distance to CPA: 150–250 m; and
- Propagation correction :  $18\log(r)+5$  dB.

**[11] AQUO Project D3.1, Measurements, European URN Standard Measurement Method, 2014**

Procedure developed by TSI in the scope of AQUO Project

- Different variants (accuracy grade, deep or shallow waters) with corresponding array geometry;
- Recommends different measurement distances and several ship passages, whose results are combined; and
- Possibility to determine directivity of radiated noise.

**[12] National Physical Laboratory, Good Practice Guide No. 133, Underwater Noise Measurement, 2014**

Provides guidance for underwater radiated noise measurements, including radiation noise from ships. This document provides recommendations for both deep and shallow waters (see also references [1] and [2]) but doesn't replace a standard procedure document. It also includes a section on the determination of propagation loss in shallow waters, which can be quite useful.

**[13] RINA, Amendments to Part A and Part F of - Rules for the Classification of Ships - New additional class notation: -DOLPHIN QUIET SHIP and -DOLPHIN TRANSIT, 2017**

Procedure recommended by the RINA for the determination of underwater ship radiated noise. Based on ISO 17208-1, only deep waters (greater than 200 m).

**[14] Lloyd's Register - ShipRight Design and Construction - Additional Design and Construction Procedure for the Determination of a Vessel's Underwater Radiated Noise, February 2018**

Procedure recommended by the Lloyd's Register for the determination of underwater ship radiated noise.

- For deep waters, based on the ISO 17208-1;
- Correction to surface reflection in deep waters: simple formula; and
- Shallow waters: Use of an array of 3 hydrophones at specified depths. The correction factors for the three locations are estimated using numerical models (wavenumber integration method is recommended below 1000 Hz).



**[15] ABS, Guide for the classification notation – underwater noise. American Bureau of Shipping, July 2018**

The measurement configuration in deep waters is similar to the one specified in ISO 17208-1. Measurement in shallow waters is cited (water depth greater than 60 m and smaller than 150 m) but the measurement configuration is not detailed in that case. Distance correction is applied for each hydrophone: propagation loss can be obtained by the measurement, numerical calculation or simple propagation law (spherical spreading).

**[16] CCS, Guideline for Underwater Radiated Noise of Ships, 2018**

<https://www.ccs.org.cn/ccswzen/font/fontAction!article.do?articleId=4028e3d66daf3189016f3fe9371e04cd>

**[17] Bureau Veritas Rule Note NR614, Underwater Radiated Noise (URN), 2014 (revised version in 2018)**

Procedure recommended by Bureau Veritas for the determination of underwater ship radiated noise.

- Based on the procedure defined in AQUO project, with 2 runs at 3 distances;
- Deep or shallow waters (water depth greater than 200 and 60 m, respectively);
- Vertical line of three hydrophones with specified geometry;
- Distance correction: obtained from numerical modelling or a simplified analytical formula; and
- Two options: With or without correction for Lloyd's mirror effect.